VERTICALLY PROPAGATING WAVES IN A NUMERICAL STRATOSPHERIC MODEL

by

MICHAEL HENRY KIRKISH

B.S., University of California, Davis
(1977)

SUBMITTED IN PARTIAL FULFILLMENT
OF THE REQUIREMENTS FOR THE
DEGREE OF

MASTER OF SCIENCE

at the

MASSACHUSETTS INSTITUTE OF TECHNOLOGY

(DATE: JUNE, 1979)

Signature of Author.....
Department of Meteorology, June 29, 1979

Certified by.....
Thesis Supervisor

Accepted by.....
Chairman, Department Committee

VERTICALLY PROPAGATING WAVES IN A NUMERICAL STRATOSPHERIC MODEL

by

MICHAEL HENRY KIRKISH

Submitted to the Department of Meteorology
on June 29, 1979 in partial fulfillment of the requirements
for the Degree of Master of Science

ABSTRACT

Vertically propagating planetary scale waves are an important feature of the wintertime stratospheric and mesospheric dynamics. The waves, particularly zonal wavenumbers 1 and 2, are analyzed in the quasi-geostrophic chemical-dynamical numerical stratospheric model developed at M.I.T.

It appears that zonal wavenumbers 1 and 2 in the model propagate energy more rapidly through the winter stratosphere than those which are observed. Above the stratopause there is little or no propagation of energy by the model waves in disagreement with observed wintertime quasi-geostrophic waves. The latter may be due to wave reflection at the rigid lid upper boundary of the model. It is likely that the former is due to the inability of the model to precisely simulate the wintertime mean circulation. It is shown that vertical propagation of planetary scale mid latitude eddies is quite sensitive to the zonal wind configuration.

In the final section, wave-zonal interactions are

qualitatively discussed by examining spatial derivatives of two eddy fluxes. It is found that most conversions between quasi-geostrophic eddies and the zonal flow occur in the vicinity of the jets.

Thesis Supervisor: Ronald Prinn, Associate Professor

CONTENTS

1. INTRODUCTION

The wintertime stratospheric dynamics are predominantly composed of a mean zonal state upon which are superimposed vertically propagating long wave disturbances excited in the troposphere.

The manner in which these waves propagate in a numerical dynamical-chemical model is investigated and compared with observation. The phases and amplitudes of the first three wavenumbers are examined and a refractive index is defined in order to understand horizontal and vertical eddy propagation processes within the model. Wave-zonal interactions in the model are discussed using two eddy flux terms which are easily computed for the model but which are difficult to obtain accurately for the real atmosphere.

2. WAVES IN THE WINTER STRATOSPHERE

In vertical cross-section, the atmosphere is divided into a number of well-defined layers in which the sign of the lapse rate is roughly constant. The lowest layer is the troposphere, a region in which temperature decreases with height to a minimum at the tropopause (elevation ranges between 10 and 18 km and is a function of season and latitude). Above this level is the stratosphere where temperatures increase with height, except in the lower stratosphere which is nearly isothermal. Stratospheric temperatures reach a maximum at the stratopause (elevation approximately 50 km). Thus, the stratosphere is a region of high static stability.

Tropospheric motions are made up of a myriad of mean flows and various long and short wavelength perturbations. In contrast, the stratospheric circulation is principally made up of long planetary waves superimposed upon the mean zonal flow. This long wave activity is observed to be at a maximum during the winter months at mid latitudes. For this reason, this paper is primarily concerned with the wintertime stratosphere.

Figure 2.1 gives a typical winter mean of the zonally averaged temperature field. It is apparent that the lower stratosphere is coldest above the equator, cool near the winter pole, and warmest at the summer pole. The higher stratosphere has temperature maximums above the tropics and

the summer pole, with a minimum at the winter pole. There is a slight asymmetry in the location of the equatorial maximum which is actually centered at about 15^{o} into the winter hemisphere.

Figure 2.2 gives a representation of the meridional cross section of the mean zonal wind (from Newell, 1968) at the solstices. Positive wind values are westerlies. The winter hemisphere is a region of strong stratospheric westerlies which reach a maximum in the polar night jet centered approximately at 40^{o} latitude and 60 km altitude. There is an easterly jet in the corresponding location in the summer hemisphere. In fact, easterlies prevail throughout most of the summer stratosphere and extend 10^{o}-20^{o} across the equator. There are, however, weak westerlies toward the summer pole which extend as far as 20^{o} in the troposphere and lower stratosphere. These are mirrored by stronger westerlies in the winter hemisphere at approximately the same location. The main features of the mean meridional circulation for January were deduced by Vincent (1968). His results showed a two cell structure in the Northern Hemisphere. The tropical Hadley cell extends into the stratosphere where it carries air across the equator to mid latitude sinking regions. Likewise, polar air rises in a Ferrel cell and is carried across high latitudes to the same mid latitude sinking areas.

It is now apparent that the troposphere is a primary energy source for the stratosphere. Starr (1960) suggested this might be the case, rather than the idea that stratospheric energy is internally generated. Newell (1966) summed up the evidence in favor of tropospheric forcing. Oort (1964) used the box notation of Lorenz (1954) to estimate the energy cycle of the atmosphere for the IGY. He concluded that work done by tropospheric eddies causes the stratospheric energy cycle to proceed in the reverse direction of the one in the troposphere. That is, in the troposphere, solar heating creates mean available potential energy (PE) which gives rise to eddy PE which proceeds to eddy KE (baroclinic waves) and subsequently mean KE which are dissipated by friction. Conversely, the lower stratospheric energy cycle proceeds as follows:

1. Work done by tropospheric eddies at 100 mb creates eddy KE in lower stratosphere.
2. Conversion of eddy KE to eddy PE (by cold air rising, warm air sinking) and zonal KE (by negative viscosity mechanism).
3. Counter gradient transport of heat by the eddies converts eddy PE to mean zonal PE.
4. Mean zonal PE is dissipated by radiation.

In a later study, Dopplick (1971) included radiative effects in calculating the lower stratospheric energy cycle for 1964. His results resembled Oort's somewhat in sign

and order of magnitude, with the exception that Dopplick found a net conversion of mean zonal PE to eddy PE. He attributed the discrepancy to the fact that Oort chose different horizontal and vertical boundaries in his study.

Dopplick was able to conclude that winter eddies in the lower stratosphere are maintained by the release of eddy PE and absorption of tropospheric energy. The energy from these eddies is converted into mean zonal KE by Reynolds stresses. At higher elevations, energy propagated upward by these eddies is "fed" by a similar process into the polar night jet in order to maintain the zonal kinetic energy.

The energy cycles calculated by Oort and Dopplick are for the annual mean. However, since most of the energy conversions in the stratosphere occur in winter, their findings apply largely to the winter energy cycle.

The theoretical aspects of tropospheric forcing have been evolving along with the observational basis. Charney and Drazin (1961) investigated the propagation of energy into the stratosphere through its lower boundary by quasi-geostrophic planetary waves excited in the lower troposphere. They used beta plane theory to conclude that long waves can propagate vertically only in the region of westerly wind velocities less than the Rossby critical velovity U_c. They found U_c=38 m/sec at mid latitudes corresponding to a wave with a zonal wavelength of 14,000 km and a meridional

wavelength of 20,000 km. Dickinson (1968) studied planetary disturbances on a spherical earth. He used the Longuet-Higgins tidal theory to solve exactly the linearized vertical propagation problem away from the equator. He found the Rossby critical velocity to be increased to approximately 60 m/sec at mid latitudes for the same horizontal scales used by Charney and Drazin.

Dickinson (1969) returned to beta plane theory to investigate vertical propagation of planetary waves through an atmosphere with Newtonian cooling. Matsuno (1970) numerically solved a two dimensional quasi-geostrophic propagation equation for planetary eddies superimposed on a basic zonal flow. As a lower boundary condition he used an observed 500 mb analysis. The wavenumber 1 prdicted by his model closely resembled that of observations (Muench, 1965). His wavenumber 2 was smaller than those observed. However, Tung (1976) has pointed out that this discrepancy may be explained by the natural interannual variations of that wave since Matsuno's initial data were from a different year than Muench's observations. Van Loon et al. (1973) discussed these interannual variations for data covering a ten year period.

Schoeberl and Geller (1977) found that the vertical structures of wavenumbers 1 and 2 are very sensitive to the strength of the polar night jet and also to the type of Newtonian cooling profile used.

3. THE M.I.T. STRATOSPHERIC GCM

The quasi-geostrophic GCM developed at M.I.T. by Cunnold *et al.* (1975) provides a three-dimensional numerical laboratory in which various dynamical and chemical processes of the stratosphere can be investigated.

The model dynamics are spectral. That is, many of the important variables, i.e., streamfunction, temperature, ozone mixing ratio, vertical velocity, topography, and others, are represented as truncated series of spherical harmonics. The specified truncation is suited to the large scales present in the stratosphere, but is probably too short for tropospheric motions. When necessary, a particular field may easily be converted from spectral form to a grid point representation or vice-versa.

The equations used in this model are a form of the balance equations of Lorenz (1960). Topography, heating, and frictional effects are included as forcing terms. Ozone heating is computed exactly at upper levels. Otherwise, heating is parameterized using an empirical Newtonian cooling coefficient. The global mean temperature and stability are specified rather than computed. Additionally, vertical eddy diffusivities are specified in order to model subspectral transports.

The model extends in the vertical from the surface to a rigid lid at 71.7 km. Horizontally, it ranges from

pole to pole, but with the topography of the Southern Hemisphere given as a mirror image of the Northern Hemispheric surface. Consequently, the Southern Hemisphere is in no way simulated by the model. Rather, the grid point representation of any field below the equator actually belongs to the Northern Hemisphere, but is 6 months out of phase. For example, the January streamfunction grid point representation in the Southern Hemisphere is actually a field of Northern Hemispheric July values.

The model equations are integrated with time steps of one hour. The data used in the current study are primarily from Run 29 of the model, which was run for 120 days, from December 1 until March 30. Cunnold et al. (1975) and Prinn et al. (1978) contain a more complete discussion of the dynamics as well as a description of the chemistry used. Moore (1977) contains an analysis of tracer transports by planetary scale waves in the model.

4. DATA

The data come largely from two sources, namely Run 29 of the model and satellite radiance data. Both sources have provided December-January-February averages for the first three temperature waves as well as the zonal mean temperature. Wavenumbers 4, 5, and 6, which are also available from Run 29, have been left out of this study since their amplitudes are small enough to ignore (van Loon et al., 1973).

The model temperatures are calculated from the stream-function using the thermal wind relation. The temperature as a function of longitude, latitude, elevation, and time is represented as the following truncated series of spherical harmonics:

$$T(\lambda, \mu, z, t) = \sum_{n=\ell}^{N_\ell} \sum_{\ell=-L}^{L} X_{\ell,n}(t, z)\, P_n^\ell(\mu)\, e^{i\ell\lambda}$$

where:

λ = longitude

μ = sine of latitude

z = -ln(pressure/1000 mb)

t = time

L = 6

$$N_\ell = \begin{cases} 6 \text{ if } |\ell| = 0 \\ |\ell| + 5 \text{ otherwise} \end{cases}$$

$X_{\ell,n}$ = series coefficients (complex)

P_n^{ℓ} = Legendre Polynomials

ℓ = zonal wavenumber

n = degree of spherical harmonic

This can be written as:

$$T(\lambda, \mu, Z, t) = \sum_{\ell=-L}^{L} T_\ell' e^{i\ell\lambda}$$

where

$$T_\ell' = T_\ell'(\mu, Z, t) = \sum_{n=\ell}^{N_\ell} X_{\ell,n} P_n^{\ell}(\mu)$$

is the wavenumber ℓ temperature perturbation. The amplitude and phase of T_ℓ' are computed by:

$$A = \sqrt{[Re(T_\ell')]^2 + [Im(T_\ell')]^2} = amplitude$$

$$\phi = \arctan\left[Im(T_\ell') / Re(T_\ell') \right] = phase$$

and

Re( ) = Real part of ( )

Im( ) = Imaginary part of ( )

Under the given truncation, 79 complex series coefficients are output by the model per level, per day. To obtain a

seasonal mean, the phase and amplitude are computed from the time averaged T_i'. Phases and amplitudes are finally output on a grid of pole to pole latitudes versus elevation up to the lid at 71.6 km.

The model temperature waves are compared with observational data from Barnett (personal communication) which were obtained by the Nimbus 4 (launched 1970) and Nimbus 5 (launched 1972) selective chopper radiometers (SCR) and the Nimbus 6 (launched 1975) pressure modulator radiometer (PMR).

The SCR data is used to compute temperatures with a high vertical resolution up to the stratopause. Above that level, data is from the PMR, which can sound temperatures from layers as high as the mesopause. The vertical resolution of both the SCR and the PMR is roughly 10 km.

Datailed information and further references concerning the Nimbus 4 and Nimbus 5 SCR's can be found in Barnett *et al.* (1975 and 1972). Hirota and Barnett (1977) have discussed the PMR on Nimbus 6. The method of inversion used to deduce the temperatures from the measured radiances is described by Conrath (1972).

The mean zonal temperatures as well as phases and amplitudes of wavenumbers 1,2, and 3 from an average observed winter are reproduced for comparison with Run 29 data. In order to mimic the format of the model data, summertime Northern Hemispheric means have been substituted for Southern Hemispheric data.

5. PROCEDURES

Winter stratospheric planetary scale eddies can transport energy upwards from the tropopause. At higher altitudes, the eddy KE is converted to eddy PE and mean zonal KE. The manner in which zonal wavenumbers 1, 2, and 3 propagate vertically through the model is investigated and compared with observational data.

A quasi-geostrophic wave in a westerly flow can propagate energy upwards only if its phase tilts to the west with increasing altitude. Eliassen and Palm (1960) demonstrated this by showing that upward transport of energy by stationary quasi-geostrophic waves in a westerly flow is possible only if the flux of sensible heat is positive, a condition associated with a westward phase tilt.

The zonally averaged wintertime phase fields from the model are examined to determine which waves are capable of transporting energy upwards and where most of that transport occurs. The model amplitude fields are included in order to give an indication of the strength of the wave activity.

It is possible to derive an index of refraction to use in determining the regions in the winter stratosphere where most wave propagation is allowed.

Charney and Drazin (1961) derived a quasi-geostrophic wave equation on a beta plane assuming no variation of the mean zonal wind with latitude and a constant N^2 (Brunt-Vaisala frequency). Holton (1975) generalized the derivation

to include latitudinal wind shears and found the index of refraction for a region in which the quantity $(\partial\bar{q}/\partial y)/\bar{u}$ is constant, where $\partial\bar{q}/\partial y$ is given by:

$$\frac{\partial \bar{q}}{\partial y} = \beta - \frac{\partial^2 \bar{u}}{\partial y^2} - \frac{1}{\rho_0} \frac{\partial}{\partial z}\left(\frac{\rho_0 f_0^2}{N^2} \frac{\partial \bar{u}}{\partial z}\right)$$

For stationary waves, the generalized Charney-Drazin index of refraction is given by:

$$n_{CD}^2 = \frac{N^2}{f_0^2}\left\{\frac{1}{\bar{u}}\left[\beta - \frac{\partial^2 \bar{u}}{\partial y^2} - \frac{f_0^2}{N^2}\left(\frac{\partial^2 \bar{u}}{\partial z^2} - \frac{1}{2H}\frac{\partial \bar{u}}{\partial z}\right) - (k^2+l^2)\right\} - \frac{1}{4H^2}\right.$$

The derivation of n_{CD}^2 is given in the Appendix.

It is helpful to examine the accuracy of the beta plane approximation in the formulation of n_{CD}^2 by considering an index of refraction for quasi-geostrophic waves derived in spherical coordinates. Matsuno (1970) derived a two-dimensional quasi-geostrophic wave equation assuming linear motions with no friction or heating on a spherical earth. His derivation was similar to that of Charney and Drazin given in the Appendix with several exceptions. He used spherical coordinates instead of the beta plane approximation and he found it necessary (from energetics considerations) to add a higher order correction to v' in the planetary vorticity advection term.

Matsuno's equation is:

$$\frac{\sin^2\phi}{\cos\phi}\frac{\partial}{\partial\phi}\left(\frac{\cos\phi}{\sin^2\phi}\frac{\partial\Psi_k}{\partial\phi}\right) + L^2\sin^2\phi\frac{\partial^2\Psi_k}{\partial z^2} + n_m^2\Psi_k = 0$$

where Ψ_k is proportional to the disturbance energy density per unit volume, $L=2a\Omega/N$, and the refractive index squared n_m^2, is given by:

$$n_m^2 = \frac{1}{\bar{\omega}}\left\{\left[2(\Omega+\bar{\omega}) - \frac{\partial^2\bar{\omega}}{\partial\phi^2} + 3\tan\phi\frac{\partial\bar{\omega}}{\partial\phi} - L^2\sin^2\phi\frac{\partial^2\bar{\omega}}{\partial z^2}\right.\right.$$

$$\left.\left. - \frac{1}{H}\frac{\partial\bar{\omega}}{\partial z}\right]\right\} - \sin^2\phi\frac{L^2}{4H^2} - \frac{k^2}{\cos^2\phi}.$$

$\bar{\omega}=\frac{\bar{u}}{a\cos\phi}$ and the other variables are defined in the Appendix. At a constant mid latitude, $n_m^2 \approx f_o^2 a^2 n_{cD}^2/N^2 + k^2a^2$.

Matsuno's equation describes wave propagation in both the y and the z directions, and in this sense it is more useful than the Charney-Drazin formulation. However, n_m^2 contains no information about the latitudinal scale of the waves since this scale is implicit in Ψ_k. In this respect, n_m^2 is less useful than n_{cD}^2 which tends to be dominated by the meridional wavenumber term. In the present study, the index of refraction is used to qualitatively aid in describing mid latitude quasi-geostrophic wave propagation, so that either formulation would provide adequate results.

In the next section, various aspects of the wavenumber 1 indices of refraction from both Matsuno and Charney-

Drazin are examined.

A wave can only propagate vertically in regions of positive n^2, and the strength of propagation increases as n^2 increases. In regions where the refractive index squared is less than zero, only external wave modes are permissable. A vertically propagating wave will be channeled away from areas of negative or small positive n^2 and into areas where n^2 is large and positive.

The presence of a region of positive refractive index squared does not always imply vertical energy propagation there. It is necessary that an eddy of sufficient amplitude be also present and also propagating vertically.

The fields of n^2 are used in conjunction with fields of amplitude and phase to investigate the propagation properties of a given wave in a specified mean zonal wind distribution.

Note that the indices of refraction used in this study come from quasi-geostrophic theory which is most valid away from the equator and away from the polar night jet. Consequently, the fields of n^2 will be used to indicate in a qualitative sense the region where vertical propagation is most probable.

6. ANALYSIS

The zonal mean temperature for winter from Run 12 of the model was compared with a typical observed zonal temperature (Newell, 1968) by Cunnold et al. (1975). There is reasonable agreement between the two with the following exceptions. The model lacks the observed wintertime mid latitude warm belt in the lower stratosphere. In addition, the model overpredicts the pole-to-pole temperature gradient near the stratopause.

I. Phase and amplitude fields

The phases and amplitudes of wavenumber 1 from the model and from satellite observations are shown in Figures 6.1 and 6.2. In both instances, the phases clearly tilt to the west at mid and high latitudes in the winter hemisphere, although this tilt is far steeper in the model. For example, at 50° in both figures the phase is 180° at about 9 km. At 40 km, the model phase has rotated a full 360° while the observed phase has only tilted west to about 60°. Indeed, the observed phase rotates a total of 180° from the tropopause to 70 km.

It is significant that the model phase becomes more or less constant above the level 40-45 km. This situation presumably is due to total wave reflection and perhaps subsequent interference from the rigid lid at 71.7 km.

This reflection phenomenon points to what may be a major defect of current stratospheric models, i.e. the inability to correctly model the upper boundary.

The top of the atmosphere provides a serious challenge to a numerical simulation since it has no convenient finite lid through which energy propagation is forbidden. However, a wave incident at the rigid lid of a model may be totally reflected downwards so that it interferes with upward propagating waves.

Cardelino (1978) used several simple numerical models to examine the upper boundary problem. He concluded that wave reflection at the upper boundary of a GCM could be reduced by improving the vertical resolution, by raising the lid to a level where Newtonian cooling has sufficiently damped the wave, or by somehow creating an artificial sponge layer at the top of the model in which incident waves are damped to zero. The feasibility of integrating one or more of the alternatives into the model is currently being studied at M.I.T. (F. Alyea, personal communication).

The lower troposphere, particularly near the winter pole is another problem area in the model. However, this is not too important since the model is principally concerned with simulating higher regions of the atmosphere.

The observed phase is nearly constant with height throughout most of the winter troposphere. At higher levels,

a waveguide, bounded by the winter pole and the line at which the phase begins to tilt westward, is formed. The maximum of the observed wave amplitude (Figure 6.4) is well within the bounds of this waveguide, as is the polar night jet. Presumably, eddy kinetic energy is propagated through the waveguide to upper regions where it is available to feed the zonal flow at the level of the jet. No similarly defined waveguide is found in the model phase map. Rather, the waves are propagating upwards everywhere in mid latitudes up to about 40 km.

A comparison between Figures 6.3 and 6.4 shows a maximum in the model wavenumber 1 amplitude field centered at roughly the same location as the single observed maximum. Additional model amplitude maximums occur at winter mid latitudes above the stratopause and in the summer hemisphere in the region of the line of zero zonal wind. The latter are probably due to the inability of the model to correctly locate the critical line between westerly and easterly flow. This will be discussed later on in this section.

In both the model and observed fields the wave amplitude is negligible in the presence of easterlies. This is true for all wavenumbers.

The phase of wavenumber 2 (Figures 6.5 and 6.6) bears some resemblance to that of wavenumber 1. The observed phase again tilts a total of about 180^{o} to the west from about 15 km to 70 km at winter mid latitudes, though a smooth

waveguide is not present. The model phase tilts about 250° -300° westward within the stratosphere and again becomes nearly constant above the stratopause.

In both cases, the channel of westward phase tilt is narrower for wavenumber 2 than for the longer wave.

Figure 6.8 shows the observed amplitude of wavenumber 2 reaching a maximum centered near 60° at about 40 km. There is a model maximum just south of this. The model has other maximum areas in the vicinity of the tropopause as well as in the constant phase region at higher elevations.

The wave amplitudes from both data sets decrease as the wavenumber increases. The maximum points in the wavenumber 2 fields are about one-fourth as large as those in the wavenumber 1 fields. Again the region of small amplitude (less than .2 degrees) is bounded roughly by the line of zero zonal flow.

Figures 6.11 and 6.12 show the trend continuing in the amplitude fields of wavenumber 3. Small amplitudes cover over half of each field. There is no sign of vertical propagation in the observed phase field (Figure 6.10) and only a slight westward tilt in the mid latitude model winter hemisphere (Figure 6.9). It appears the assumption that wavenumbers 1 and 2 are the dominant internal modes in the winter stratosphere is valid.

II. Analysis of the refractive index squared

Charney and Drazin found that in the absence of wind shear, vertical propagation of the long planetary waves being considered in this study is forbidden wherever the zonal wind is greater than 38 m/sec. However, inspection of $n_{c_0}^2$ shows that trapping by the zonal flow could be decreased or increased by the shear terms in $\partial\bar{q}/\partial y$. Vertical propagation is allowed only if:

$$\frac{1}{\bar{u}}\left[\frac{N^2}{f_o^2}\beta - \frac{N^2}{f_o^2}\frac{\partial^2\bar{u}}{\partial y} - \frac{\partial^2\bar{u}}{\partial z^2} + \frac{1}{2H}\frac{\partial\bar{u}}{\partial z}\right] > (k^2+l^2)\frac{N^2}{f_o^2} + \frac{1}{4H^2}$$

(see Appendix for definitions of variables)

Figure 6.13 illustrates this criterion at 40°N, 50°N, and 60°N. At all three latitudes, the variation of potential vorticity with latitude is generally positive and is greater than the magnitude of the sum of the other three terms in $n_{c_0}^2$ at many levels. It is notable that the $\partial\bar{q}/\partial y$ term tends to decrease with height due to the increase with height of $\bar{u}$.

Note also that the latitudinal wavenumber term dominates the zonal wavenumber term at all three latitudes. This is an indication that the meridional scale of a wave can be more important in determining its propagation properties than the zonal scale.

Figures 6.14, 6.15, and 6.16 show the effects of wind shear in greater detail by comparing the various terms which make up $\partial\bar{q}/\partial y$ at three latitudes. Beta is generally

the largest term, though the shear terms are far from insignificant.

The behavior of $(\partial\bar{u}/\partial z)f_c^2N^{-2}H^{-1}$ is fairly predictable. At 40°N and 50°N it is positive in the troposphere and negative at the level of the lower stratospheric jet. It becomes positive above the jet and remains positive up to the level of the polar night jet. The profile at 60°N is similar except $\partial\bar{u}/\partial z$ does not become negative at the lower stratospheric jet. This term is generally the least significant of the shear terms.

At all three latitudes, $-\beta^2\bar{u}/\partial y^2$ is nearly zero between the surface and the 20 km level, indicating a constant decrease of $\bar{u}$ with latitude in that region. At 40°N it is small and positive up to 40 km and is large and positive above that level. A maximum is reached at roughly 50 km, where this term is the largest in $\partial\bar{q}/\partial y$. At 50°N, $-\beta^2\bar{u}/\partial y^2$ is positive above 20 km and attains its greatest magnitudes above the 55 km level where it is slightly less than beta. At 60°N, $-\beta^2\bar{u}/\partial y^2$ is less than zero above 20 km and ranges in magnitude between 20% and 80% of beta.

At the three latitudes, $-f_c^2N^{-2}(\partial^2\bar{u}/\partial z^2)$ oscillates between large positive and large negative values particularly at the levels of the jets where large changes in $\partial\bar{u}/\partial z$ are taking place, and also at intermediate levels. $-f_c^2N^{-2}(\partial^2\bar{u}/\partial z^2)$ is responsible for the prominant minimum at 20 km and 20°N

and 50^{o}N in Figure 6.13.

Apparantly the zonal wind configuration is vitally important in increasing and decreasing the trapping properties of the atmosphere. In order that mid latitude quasi-geostrophic waves be allowed to propagate upwards, $N^2 f^{-2} \bar{u}^{-1} (\partial \bar{q}/\partial y)$ must be positive and greater than the magnitude of the sum of the other three terms in the refractive index. The importance of the zonal wind configuration is seen in two ways. First, an increase in $\bar{u}$ causes a decrease in the magnitude of the positive contribution to n_{co}^2 ($-k^2$, $-l^2$, and $-1/(4H^2)$ are all negative). This is obvious from an inspection of Equation 12 in the Appendix and it implies that the effect of a jet on vertical propagation is to increase the trapping properties of the atmosphere in its vicinity. Secondly, the horizontal and vertical variations in the zonal wind can increase or decrease trapping through their effect in $\partial \bar{q}/\partial y$. It has been shown that the terms in $\partial \bar{q}/\partial y$ which include these variations can be significant in affecting the sign of n_{co}^2.

The non-dimensional index of refraction squared derived by Matsuno is compared with its dimensional counterpart from Charney-Drazin theory in Figures 6.17 and 6.18 respectively. The wintertime mean zonal wind from the model (Figure 6.19) and a typical winter mean flow (Figure 2.2) were used in the computations.

Along the line of zero zonal velocity there is a

singularity in the index of refraction which is clearly visible in the different fields for both data sets. Additionally, both formulations show a minimum of n^2 in the region of the lower stratospheric jet, although this minimum area is weaker in Matsuno's. The fields of n^2 show a steady increase upward and equatorward above 30 km.

The major differences occur near the winter pole, particularly at higher altitudes where the region of negative index of refraction squared is much wider for the Charney-Drazin formulation. In the forthcoming analysis, n_m^2 will be used since it gives insight into both horizontal and vertical eddy propagation.

Matsuno's index of refraction for wavenumber 1 from the model is now compared with observation (Figure 6.17). As previously mentioned, there is a minimum of n_m^2 in the region 10-20 km. This area acts to block propagating waves and channel them toward higher n_m^2 values. The maximum centered roughly at 65^o in the wavenumber 1 amplitude fields may be due to the blocking action of this minimum which inhibits the energy from propagating southward.

The minimum region in the model is somewhat distorted, due mainly to the location of the line of zero zonal wind which extends into the model summer hemisphere at 20 km. The observed line of zero wind velocity is totally contained within the winter hemisphere. Presumably the discrepancy is due to the absence in the model of wavenumbers beyond 6,

which transport momentum away from the equator in the real atmosphere. The incursion of westerlies into the model summer hemisphere causes the minima to extend across the equator, to regions where the observed n_m^2 is negative and large.

Furthermore, the extension of the line of zero zonal flow to as far north as 35^o is significant (due to the presence of $\bar{u}$ in the equation for n_m^2)and it acts to decrease the trapping properties of the atmosphere.

The distortion of the minimum could explain the excessive westward tilt of the model waves at stratospheric mid latitudes. The observed n_m^2 field shows a high latitude channel of larger values between two minima at roughly 25 km which would "guide" an upward propagating wave to higher altitudes. The model refractive index has no such detail.

A further disagreement occurs near the pole where there is an area of singularity at 25-30 km in the model field which the observed field lacks. This is due to the small zone of easterlies found at that location in the model.

Otherwise, the model and observed fields show good agreement. There is the upward and equatorward increase of n_m^2 above 30 km in both, and both display a region of trapping at higher altitudes near the pole.

It appears a mid latitude wavenumber 1 disturbance propagating out of the winter troposphere is forced to higher latitudes in the lower stratosphere. Further prop-

agation is predominately directed upwards and to the south. This view fully agrees with the previous analysis of the phase and amplitude of wavenumber 1. Both the model and observed fields showed a concentration of vertically propagating wave energy centered at high latitudes in the lower stratosphere and distinctive westward phase tilts at mid to high latitudes. At higher latitudes, the observed phase ceases to tilt westward below mid latitudes, yet this is the region in which the refractive index squared assumes its highest values. Apparently, stationary waves incident at the line of zero zonal velocity are absorbed into the zonal flow (Booker and Bretherton, 1967).

7. CONVERSION OF EDDY KINETIC ENERGY TO MEAN ZONAL KINETIC ENERGY IN THE MODEL

The purpose of this section is to provide some insight into the manner in which kinetic energy propagated upwards by the planetary scale quasi-geostrophic waves in the model is released into the zonal flow.

The notation used is as follows:

$((A)) = (2\pi)^{-1}\int_0^{2\pi} A \, d\lambda$	zonal mean
$A^* = A - ((A))$	departure from zonal mean
$\bar{A} = T_o^{-1}\int_0^{T_o} A \, dT$	time mean (T_o=3 months)
$A' = A - \bar{A}$	departure from time mean

The two eddy fluxes which will be examined are $\overline{((w^*u^*))}$ and $\overline{((v^*u^*))}$. In the real atmosphere, these quantities are extremely difficult to measure. However, in this spectral model, it is a simple matter to compute them accurately.

$\overline{((w^*u^*))}$ is the vertical flux of zonal momentum by all the eddies and is shown in Figure 7.1 for a winter-summer average. The following discussion refers to the winter hemisphere. There is a strong center of positive $\overline{((w^*u^*))}$ at low latitudes at about the level of the stratopause. This is roughly the location of the lower stratospheric jet. Below this level, there are centers of negative $\overline{((w^*u^*))}$ at both low and high latitudes. There is a line of zero $\overline{((w^*u^*))}$ which extends through the stratosphere

from the equator to the pole. At higher altitudes, this flux reaches a negative maximum at lower latitudes near the level of the polar night jet. To the north of this region is an area of positive vertical eddy momentum flux which extends into the jet. Further north (60^{o}N) at an altitude of roughly 40 km is another center of negative $\overline{((w^{*}u^{*}))}$.

The horizontal flux of momentum, $\overline{((v^{*}u^{*}))}$, for the same 3 month period is shown in Figure 7.2. This flux is positive nearly everywhere in the winter hemisphere and has its greatest values at the lower stratospheric jet and the polar night jet. There is also a strong mid latitude maximum at roughly 35 km altitude. Near the equator, $\overline{((v^{*}u^{*}))}$ is small.

The significance of these flux diagrams can best be understood by examining the x-component of the frictionless primitive equations of motion in spherical coordinates. The following exercise follows Holton (1975). Consider:

$$(7.1)\quad \frac{\partial u}{\partial t} + \frac{\partial u^{2}}{\partial x} + \frac{1}{\cos^{2}\phi}\frac{\partial}{\partial y}(uv\cos^{2}\phi) + \frac{1}{\rho_{o}}\frac{\partial}{\partial z}(\rho_{o}wu)$$

$$- 2\Omega v\sin\phi = -\frac{\partial \Phi}{\partial x}$$

The variables in the above equation have their usual meteorological definitions.

If Equation 7.1 is linearized and zonally averaged, the following result is obtained:

$$(7.2)\quad \left(\frac{\partial}{\partial t} + ((v))\frac{\partial}{\partial y} + ((w))\frac{\partial}{\partial z}\right)((u)) - \left(2\Omega + \frac{((u))}{a\cos\phi}\right)((v))\sin\phi = -((F_{x}))$$

where,

$$(7.3)\quad \langle\langle F_x \rangle\rangle = \frac{1}{\cos^2\phi}\frac{\partial}{\partial y}\left[\langle\langle v^*u^*\rangle\rangle \cos^2\phi\right] + \frac{1}{\rho_0}\frac{\partial}{\partial z}\left[\rho_0 \langle\langle w^*u^*\rangle\rangle\right]$$

The left side of Equation 7.2 represents the total change in space and time of the zonal flow. The right hand side involves horizontal and vertical gradients of the eddy fluxes, $\overline{((v^*u^*))}$ and $\overline{((w^*u^*))}$. Thus, it can be seen from Equations 7.2 and 7.3 that these eddy flux terms can force the zonal flow. It is possible to use these two equations to qualitatively understand wave-zonal interactions in the model by estimating the derivatives of the eddy fluxes from Figures 7.1 and 7.2.

Consider first Figure 7.1. The centers of positive and negative maximums are the regions in which the vertical derivative of $\overline{((w^*u^*))}$ attains its greatest values and thus in which the greatest wave-zonal interactions are taking place. Not surprisingly, these maximum areas are primarily clustered about the jets. The smallest values of the vertical derivative of $\overline{((w^*u^*))}$ occur between the realm of the two wintertime jets, roughly between 20 km and 30 km. Similarly, in Figure 7.2, $\partial\overline{((v^*u^*))}/\partial y$ is small from 20 km to 30 km throughout the hemisphere and has its greatest values at the centers of the jets and also at mid latitudes at about 40 km, the height at which the zonal wind begins to increase with height.

On the basis of these observations it is reasonable

to assume that energy propagated upwards by the planetary scale quasi-geostrophic eddies is a significant source for both the lower stratospheric jet and the polar night jet. In order to determine the relative magnitudes of the flux terms in Equation 7.3, it would be necessary to perform a more detailed analysis.

8. CONCLUDING DISCUSSION

Long waves in the model winter stratosphere, particularly wavenumbers 1 and 2, propagate more rapidly through the stratosphere than those observed. Above the stratopause, the model waves are trapped presumably by the action of the rigid upper boundary whereas satellite observations show continued propagation through the stratopause and beyond and mid latitudes. Wavenumbers greater than 2 propagate slightly or not at all in the model upper atmosphere.

Fields of the refractive index squared, which is a sensitive function of the mean zonal flow, were considered for the case of constant Brunt-Vaisala frequency in an atmosphere with horizontal and vertical wind shears. Wavenumber 1 was seen to be channeled to the north of a minimum in the n^2 field. Further propagation was allowed upwards and to the south. The minumum was found at the level of the lower stratospheric jet which is an indication of the relationship between eddy propagation and the zonal wind shear.

It may be important that the minimum region of n^2 in the model is at a lower level and is not so extensive as the observed n^2 values which have a tongue of minima extending down into the stratosphere at mid and high latitudes. This may explain why wavenumber 1 propagates more effusely at mid latitudes in the model than through the real atmosphere, i.e., it is not so well blocked by the

zonal flow configuration as in the real atmosphere.

A qualitative analysis of the wintertime fields of ((w*u*)) and ((v*u*)) showed that most wave-zonal interactions occur within the stratospheric jets in the absence of friction.

This study was principally concerned with stationary disturbances broken up into zonal wavenumbers. It would be worthwhile to further decompose the waves into their meridional components in order to gain greater insight into wave processes in the model. A great advantage of a spectral model is that such a task can be performed with little difficulty. It would also be interesting to examine transient modes in the model.

APPENDIX

The Charney-Drazin quasi-geostrophic beta plane wave equation is generalized to include horizonatal wind shears. The following derivation from the quasi-geostrophic perturbation vorticity equation follows Holton (1975).

The important variables are:

ψ'	perturbation streamfunction
χ'	perturbation velocity potential
u'	eddy wind components
v'	
Ω	angular rotational speed of the earth
ϕ	latitude
f	$2\Omega\sin\phi$
Φ	perturbation geopotential
a	radius of the earth
H	scale height of the atmosphere = 7 km
w'	perturbation vertical velocity
ρ	density

The quasi-geostrophic perturbation vorticity equation assuming linear motions on a background zonal flow ($\bar{u}$) with $\bar{v} = \bar{w} = 0$ and no heating is:

(1)

$$\left(\frac{\partial}{\partial t} + \bar{u}\frac{\partial}{\partial x}\right)\nabla^2\psi' + \left(\frac{\partial\psi'}{\partial x}\frac{\partial}{\partial y} + \nabla^2\chi'\right)\left(f - \frac{1}{\cos\phi}\frac{\partial}{\partial y}\bar{u}\cos\phi\right) = 0$$

The beta plane approximation is now introduced. Let $f = f_o = 2\Omega\sin(\phi_o)$ = constant and $\beta = df/dy$ at ϕ_o. The Coriolis parameter is allowed to vary only in its derivatives. Substitute f and β into (1):

$$(2)\quad \left(\frac{\partial}{\partial t} + \bar{u}\frac{\partial}{\partial x}\right)\nabla^2\psi' + \left(\beta - \frac{\partial^2\bar{u}}{\partial y^2}\right)\frac{\partial\psi'}{\partial x} + f_o\nabla^2\chi' = 0$$

Assume the eddy flow is geostrophic, i. e.:

$$(3)\quad f_o\psi' = \Phi'$$

The thermodynamic and continuity equations are respectively:

$$(4)\quad \left(\frac{\partial}{\partial t} + \bar{u}\frac{\partial}{\partial x}\right)\Phi'_z + \frac{\partial\psi'}{\partial x}\frac{\partial\bar{\Phi}_z}{\partial y} + N^2w' = 0$$

$$(5)\quad \nabla^2\chi' + \frac{1}{\rho_o}\frac{\partial}{\partial z}(\rho_o w') = 0$$

Substitute (3) into (4) to get:

$$(6)\quad \left(\frac{\partial}{\partial t} + \bar{u}\frac{\partial}{\partial x}\right)f_o\frac{\partial\psi'}{\partial z} + \frac{\partial\psi'}{\partial x}\frac{\partial^2\bar{\psi}}{\partial y\partial z} + N^2w' = 0$$

Substitute (5) into (2) to get:

$$(7)\quad \left(\frac{\partial}{\partial t}+\bar{u}\frac{\partial}{\partial x}\right)\nabla^2\psi' + \left(\beta-\frac{\partial^2\bar{u}}{\partial y^2}\right) - \frac{f_o}{\rho_o}\frac{\partial}{\partial z}\left(\rho_o w'\right)=0$$

Eliminating w' between (6) and (7) and dropping the time dependence gives the quasi-geostrophic eddy potential vorticity equation:

$$(8)\quad \bar{u}\frac{\partial q'}{\partial x} + \frac{\partial \bar{q}}{\partial y}\frac{\partial \psi'}{\partial x}=0$$

and

$$(9)\quad q' = \nabla^2\psi' + \frac{1}{\rho_o}\frac{\partial}{\partial z}\left(\frac{\rho_o f^2}{N^2}\frac{\partial \psi'}{\partial z}\right) = \text{quasi-geostrophic eddy potential vorticity}$$

$$(10)\quad \frac{\partial \bar{q}}{\partial y} = \beta - \frac{\partial^2\bar{u}}{\partial y^2} - \frac{1}{\rho_o}\frac{\partial}{\partial z}\left(\frac{\rho_o f_o^2}{N^2}\frac{\partial \bar{u}}{\partial z}\right)$$

Assume solutions of the form:

$$\psi' = \Psi\, e^{i(kx+ly)} e^{z/2H}$$

Substitution into (8) yields after multiplication by $-N^2 f^{-2}\bar{u}^{-1}$ the following vertical structure equation:

$$(11)\quad \frac{d^2\Psi}{dz^2} + n_{co}^2\,\Psi = 0$$

with

$$(12)\quad n_{co}^2 = \frac{N^2}{f_o^2}\left\{\frac{1}{\bar{u}}\left[\beta - \frac{\partial^2\bar{u}}{\partial y^2} - \frac{f_o^2}{N^2}\left(\frac{\partial^2\bar{u}}{\partial z^2} - \frac{1}{2H}\frac{\partial \bar{u}}{\partial z}\right) - k^2 - l^2\right\} - \frac{1}{4H^2}\right.$$

if N^2 = constant and $\rho_o = \rho_{os}\exp(-.5z/H)$.

If n_{cD}^2 = constant, then the solution to (11) is:

(13) $\Psi = Ce^{inz} + De^{-inz}$ (C, D arbitrary constants)

For internal waves, n must be real in order to avoid infinite energy densities as z becomes infinite, so $n_{cD}^2 > 0$ is required for vertical propagation.

ACKNOWLEDGEMENTS

I would like to thank my advisor, Dr. Ronald Prinn for his valuable assistance and encouragement. I would also like to thank Drs. Fred Alyea and Derek Cunnold for their helpful advice which I sought out and received on numerous occasions. I am also grateful to Gary Moore.

I am appreciative of the support I received from my family, especially my mother and father, Vicky and Henry Kirkish, and also my sisters, Karen and Vicky M. Kirkish, and my grandmother, Mrs. Frieda Kirkish.

I would like to extend a special thank you to Lisa Simons.

This research was supported by NASA Grant NSG-2010.

REFERENCES

Barnett, J.J., M.J. Cross, R.J. Harwood, J.T. Houghton, C.G. Morgan, G.E. Peckham, C.D. Rodgers, S.D. Smith, and E.J. Williamson, 1972: The first year of the selective chopper radiometer on Nimbus 4. Quart. Journ. Roy. Met. Soc., 98, p. 17-37.

Barnett, J.J. R.S. Harwood, J.T. Houghton, C.G. Morgan, C. D. Rodgers, and E.J. Williamson, 1975: Comparison between radiosonde, rocketsonde, and satellite observations of atmospheric temperatures. Quart. Journ. Roy. Met. Soc., 101, p. 423-436.

Booker, J.R. and F.B. Bretherton, 1967: The critical layer for internal gravity waves in shear flow. Journ. Fluid Mech., 27, 513-539.

Cardelino, C., 1978: A study on the vertical propagation of planetary waves and the effects of the upper boundary condition. Master's Thesis, Department of Meteorology. M.I.T.

Charney, J.G. and P.G. Drazin, 1961: Propagation of planetary scale disturbances from the lower into the upper atmosphere. Journ. Geophys. Res. 66, p. 83-109.

Conrath, B.J., 1972: Vertical resolution of temperature profiles obtained from remote radiation measurements. Journ. Atm. Sci., 29, p. 1262-1271.

Cunnold, D., F. Alyea, N. Phillips, and R. Prinn, 1975: A three-dimensional dynamical chemical model of atmospheric ozone. Journ. Atm. Sci., 32, p. 170-194.

Dickinson, R.E., 1968: On the exact and approximate linear theory of vertically propagating planetary Rossby waves forced at a spherical lower boundary. Monthly Weather Rev., 96, p. 405-415.

Dickinson, R.E., 1969: Vertical propagation of planetary rossby waves through an atmosphere with Newtonian cooling. Journ. Geophys. Res., 74, p. 929-938.

Dopplick, T.G., 1971: The energetics of the lower stratosphere including radiative effects. Quart. Journ. Roy. Met. Soc., 97, p. 209-237.

Eliassen, A. and E. Palm, 1960: On the transfer of energy in stationary mountain waves. Geophys. Publ. 22, No. 3. 22 p.

Hirota, I. and J. Barnett, 1977: Planetary Waves in the Winter Mesosphere -- preliminary analysis of Nimbus 6 PMR results. Quart. Journ. Roy. Met. Soc., 103, p. 487-498.

Holton, J. R., 1975: The Dynamic Meteorology of the Stratosphere and Mesosphere, Boston: American Meteorological Society, 218 p.

Lorenz, E. M., 1954: The basis for a theory of the general circulation, Final Report, Part I, General Circulation Project, Department of Meteorology, M.I.T., p. 522-534.

Lorenz, E. M., 1960: Energy and numerical weather prediction. Tellus, 12, p. 364-373.

Matsuno, T., 1970: Vertical propagation of stationary planetary waves in the winter northern hemisphere. Journ. Atm. Sci., 27, p. 871-883.

Moore, G., 1977: A study of tracer transports by planetary scale waves in the M.I.T. stratospheric general circulation model. Master's thesis, Department of Meteorology, M.I.T.

Muench, H., 1965: On the dynamics of the wintertime stratospheric circulation. Journ. Atm. Sci., 22, p. 349-360.

Newell, R., 1966: The energy and momentum budget of the atmosphere above the tropopause. In Problems of Atmospheric Circulation, p. 106-126, Spartan Books, Washington.

Newell, R., 1968: The general circulation of the atmosphere above 60 km. Meteorological Monographs, Vol. 8, No. 31.

Oort, A. H., 1964: On the energetics of the mean and eddy circulations in the lower stratosphere. Tellus, 16, p. 309-327.

Prinn, R., F. Alyea, D. Cunnold, 1978: Photochemistry and dynamics of the ozone layer. Ann. Rev. Earth Plan. Sci., 6, p. 43-74.

Schoeberl, M. R. and M. A. Geller, 1977: A calculation of the structure of stationary planetary waves in winter. Journ. Atm. Sci., 34, p. 1235-1255.

Starr, V., 1960: Questions concerning the energy of stratospheric motions. Archiv. fur Meteor., Geophys. und Biokl. Ser. A, 12, p. 1-5.

Tung, K., 1976: On the convergence of spectral series--a reexamination of the theory of wave propagation in distorted background flows. Journ. Atm. Sci., 33, p. 1816-1820.

Van Loon, H., R. Jenne, and K. Labitzke, 1973: Zonal harmonic standing waves, Journ. Geophys. Res., 78, p. 4463-4471.

Vincent, D., 1968: Mean meridional circulation in the northern hemisphere lower stratosphere during 1964 and 1965. Quart. Journ. Roy. Met. Soc., 94, p. 333-349.

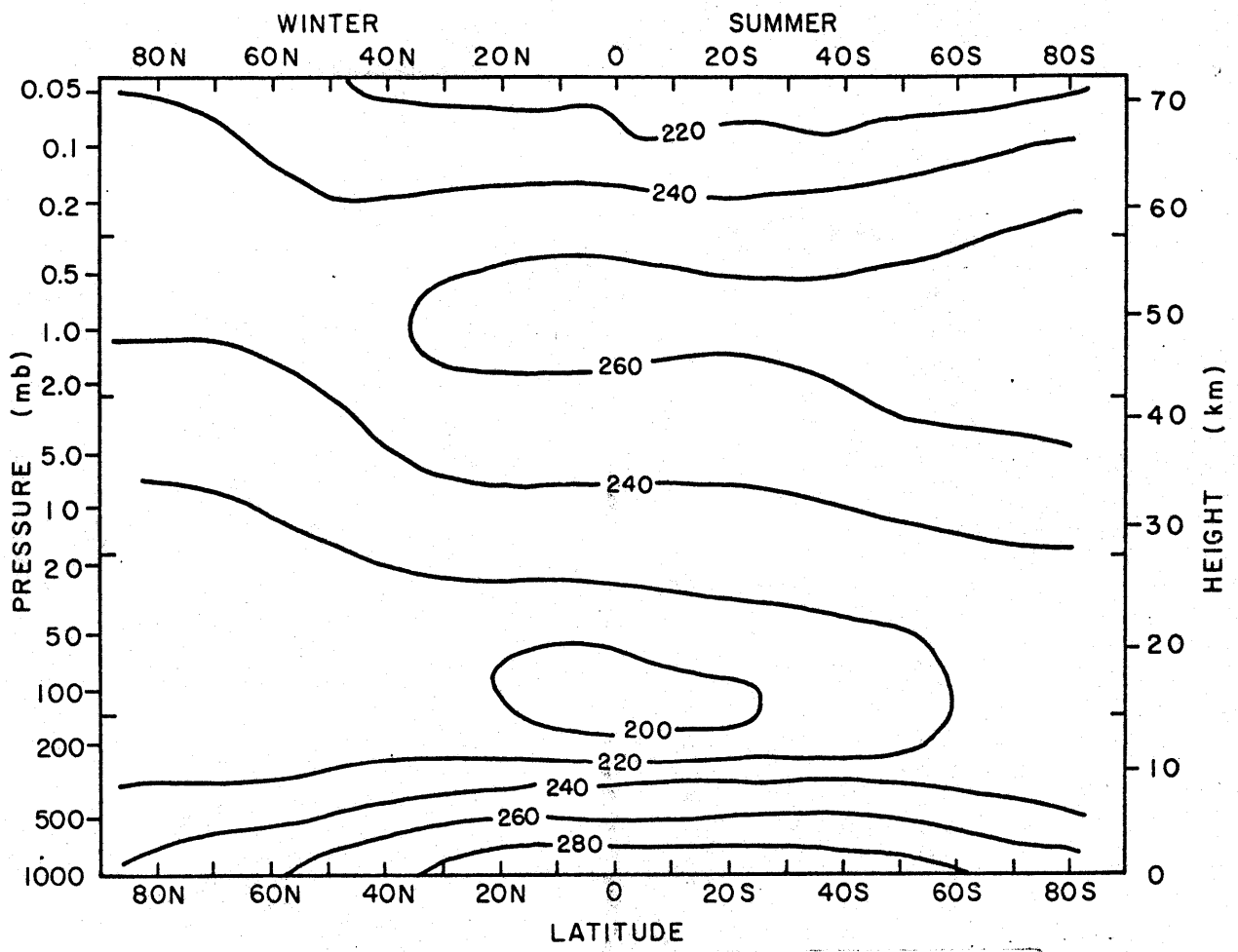

Figure 2.1: Winter-summer mean zonal temperature redrawn from Newell (1968).

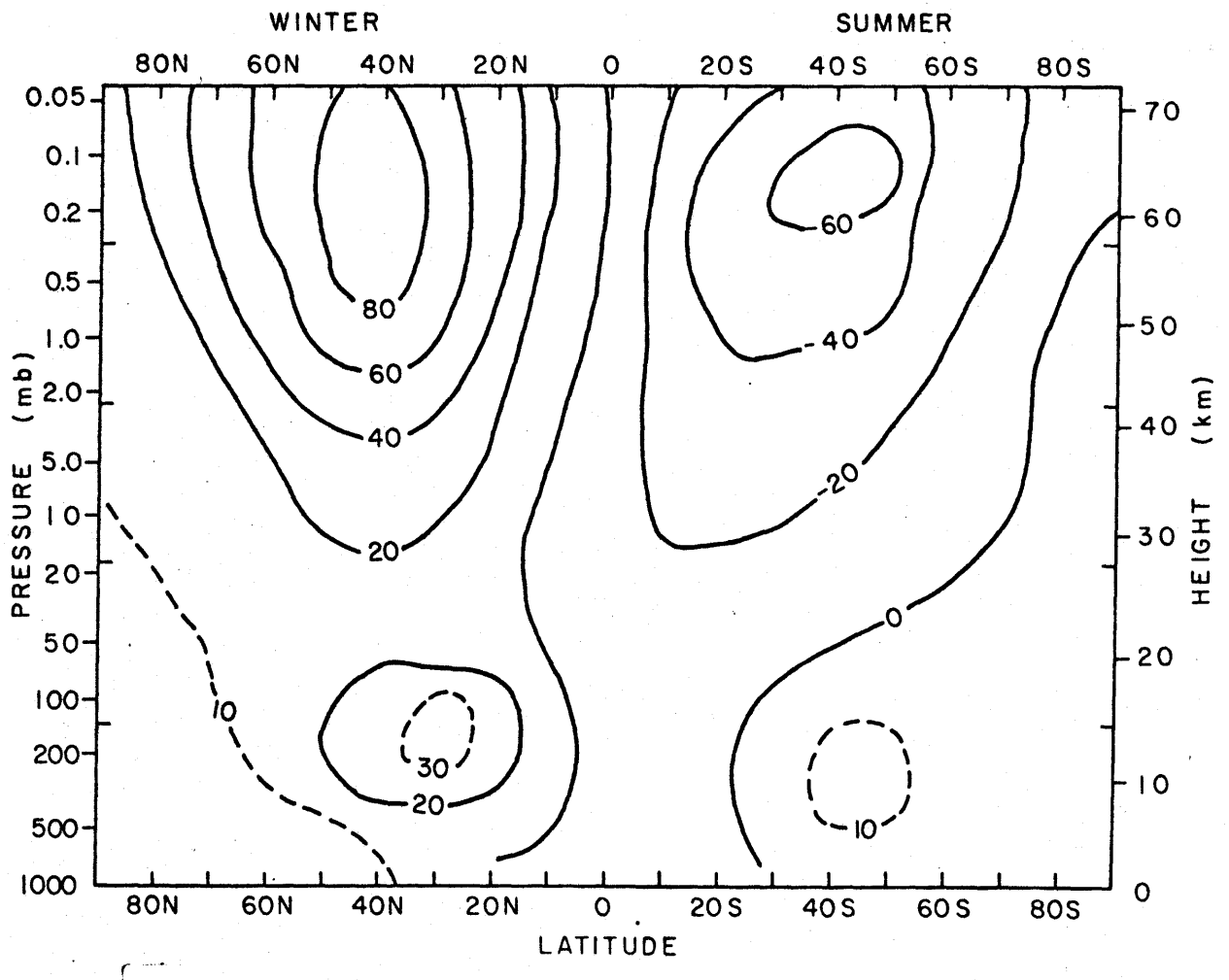

Figure 2.2: Winter-summer mean zonal wind redrawn from Newell (1968).

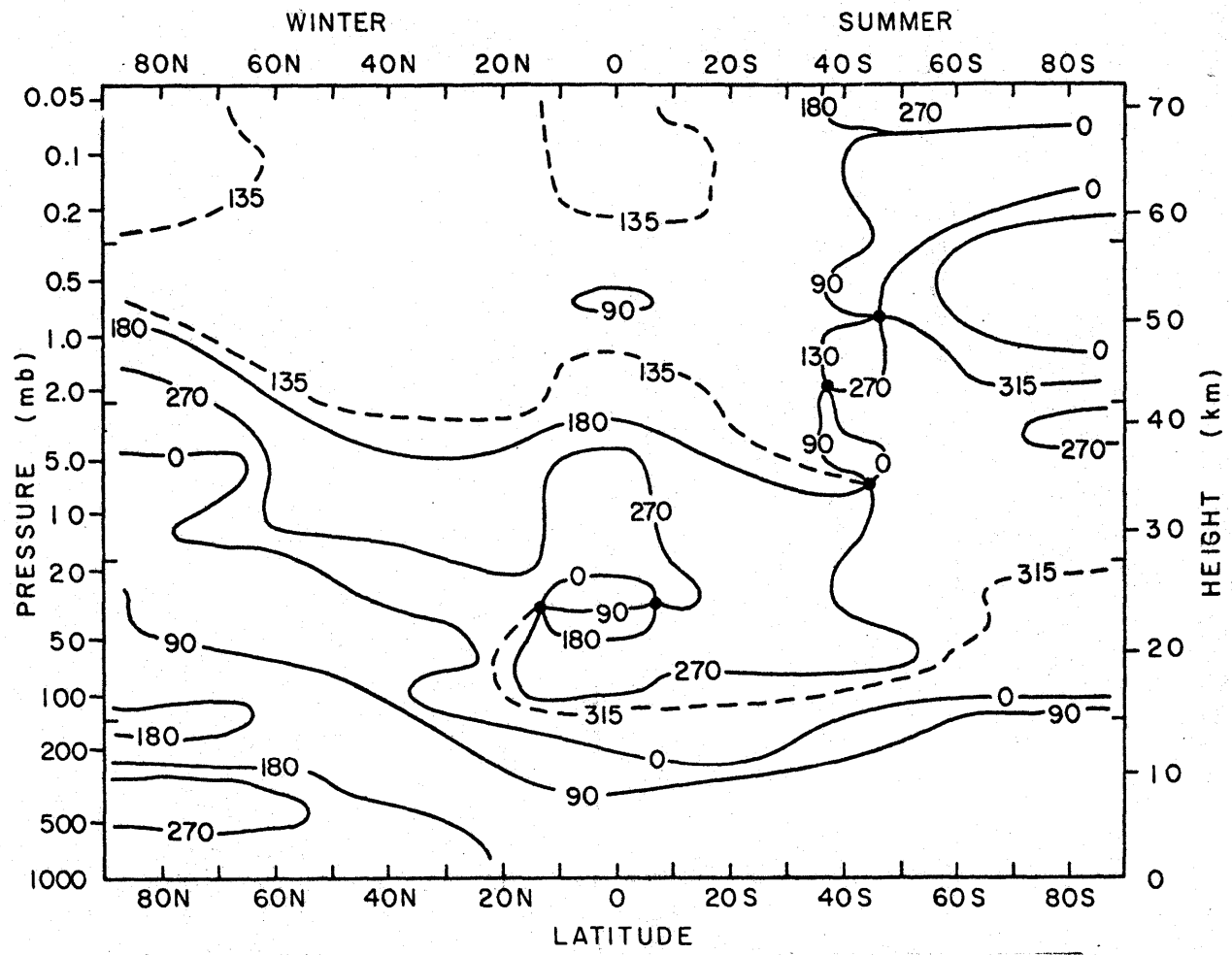

Figure 6.1: Phase (in degrees) of temperature wavenumber 1 from Run 29 (winter-summer).

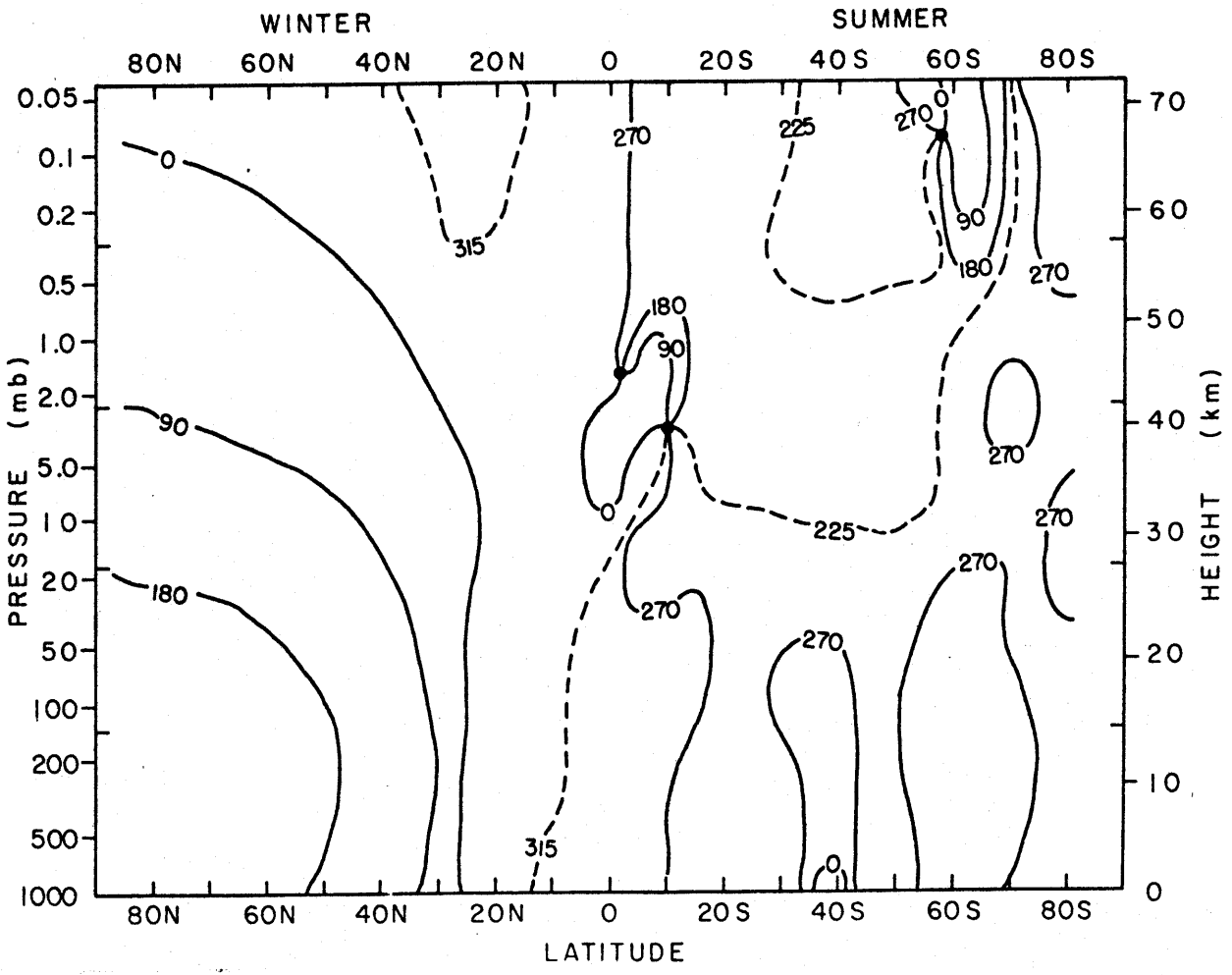

Figure 6.2: Phase (in degrees) of temperature wavenumber 1 from satellite observations (winter-summer).

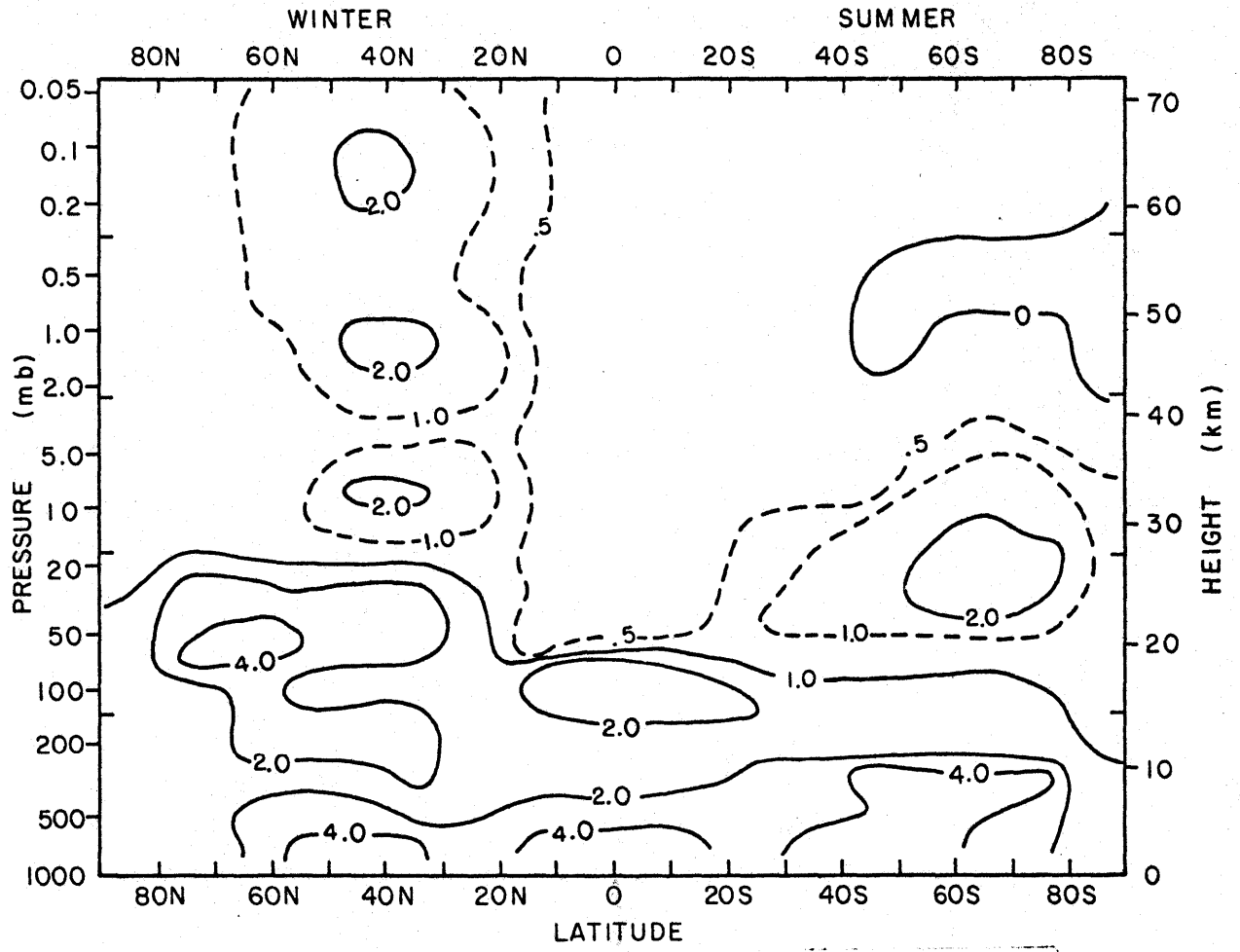

Figure 6.3: Amplitude (in degrees Celsius) of temperature wavenumber 1 from Run 29 (winter-summer).

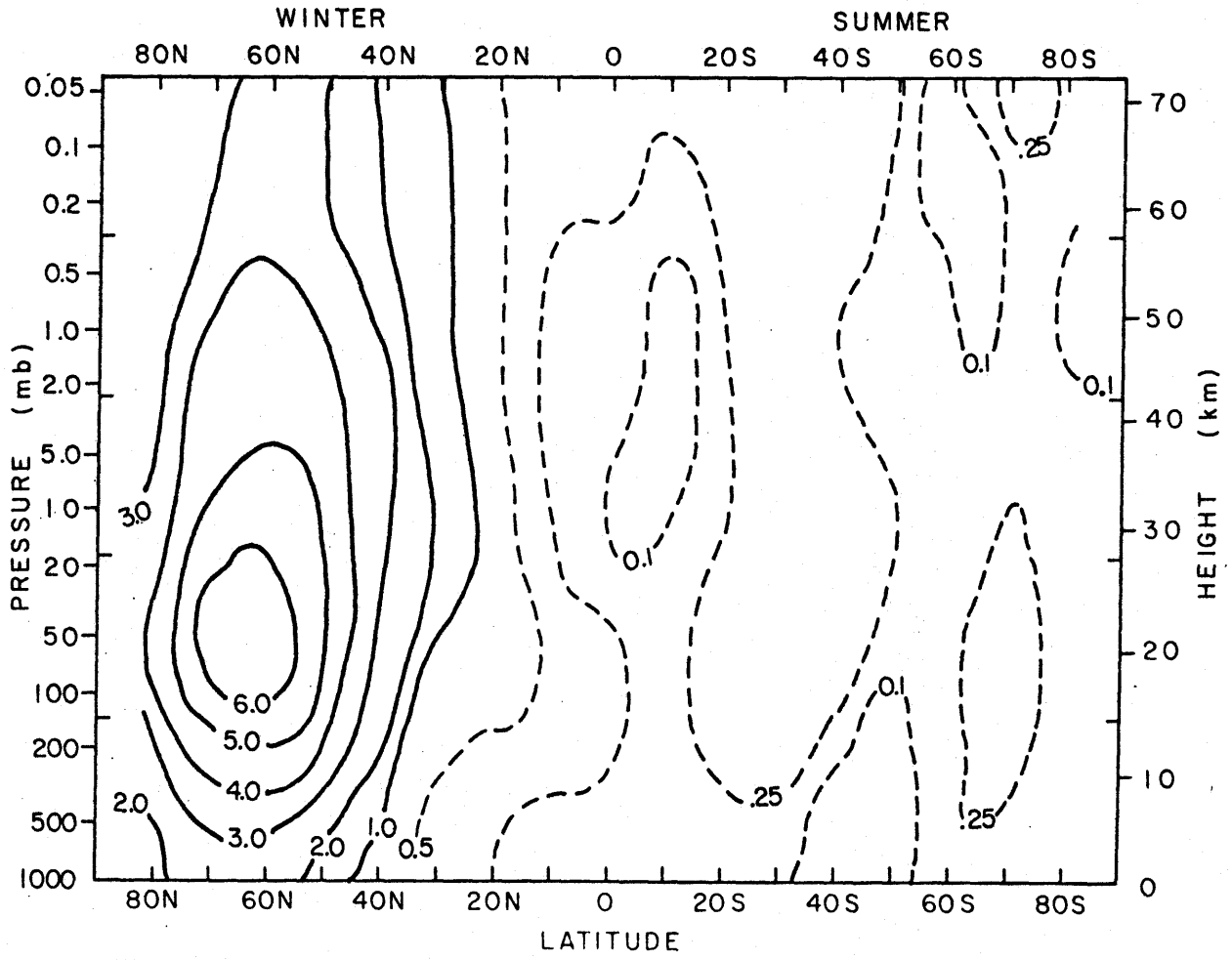

Figure 6.4: Amplitude (in degrees Celsius) of temperature wavenumber 1 from satellite observations (winter-summer).

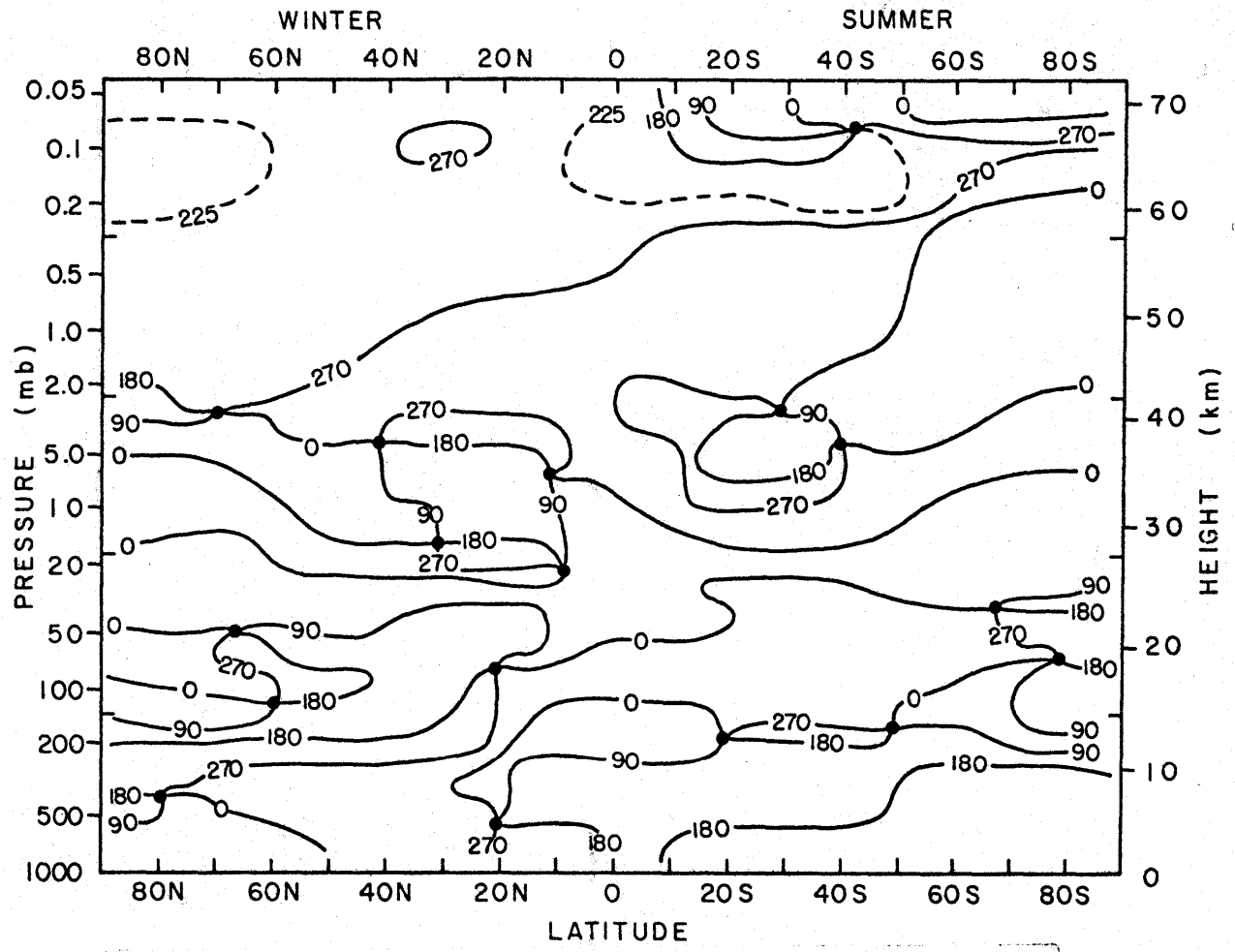

Figure 6.5: Phase (in degrees) of temperature wavenumber 2 from Run 29 (winter-summer).

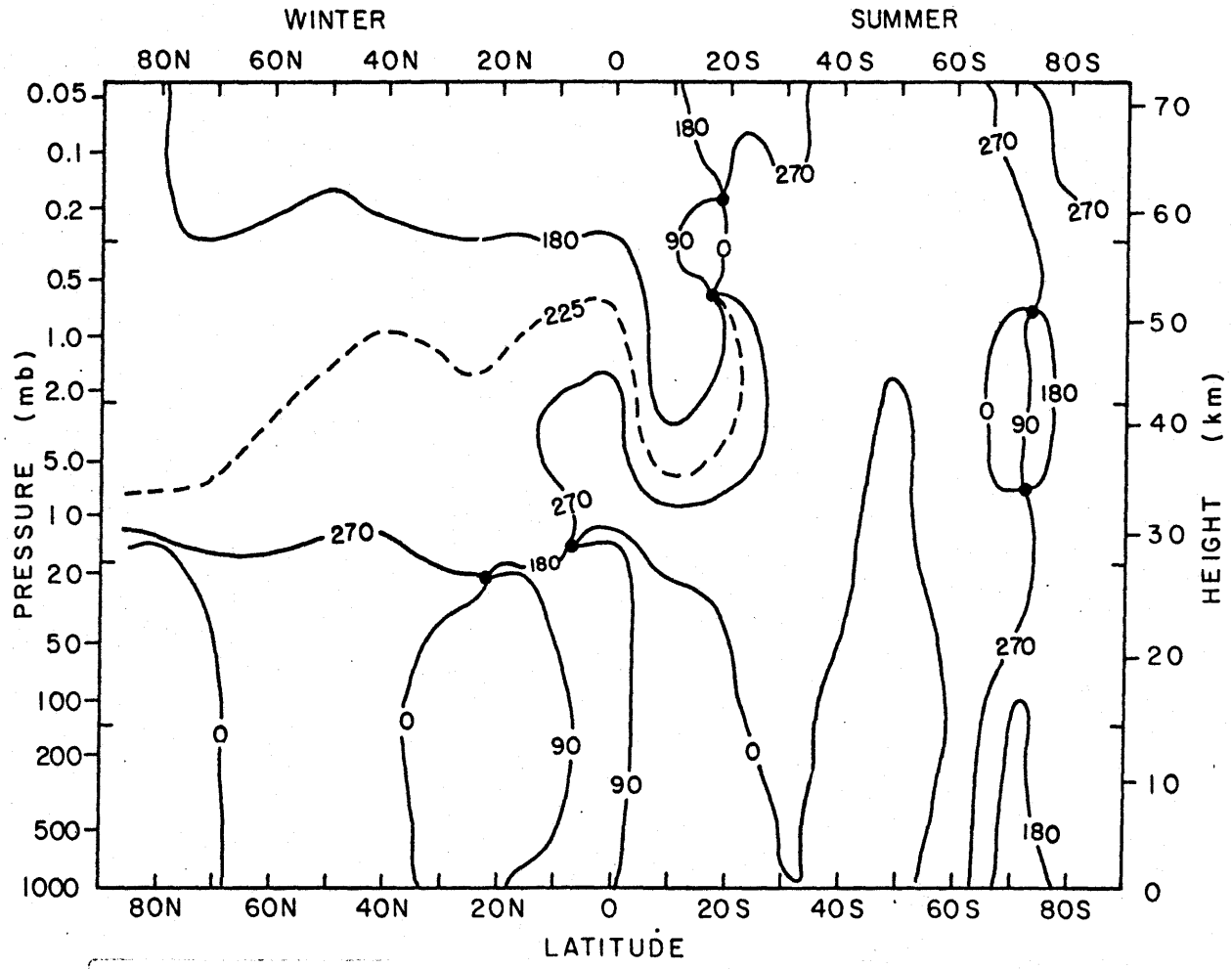

Figure 6.6: Phase (in degrees) of temperature wavenumber 2 from satellite observations (winter-summer).

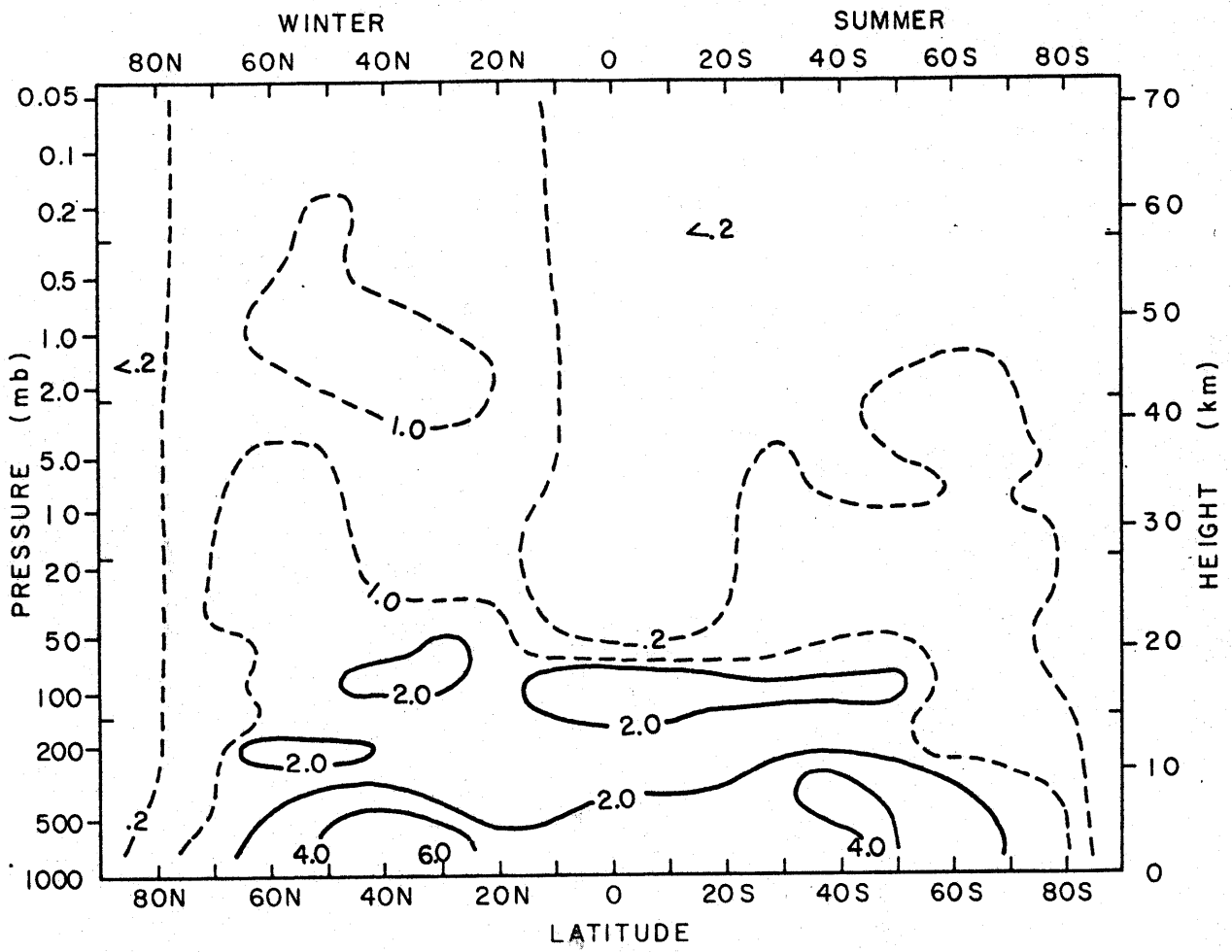

Figure 6.7: Amplitude of temperature wave-number 2 (in degrees Celsius) from Run 29 (winter-summer).

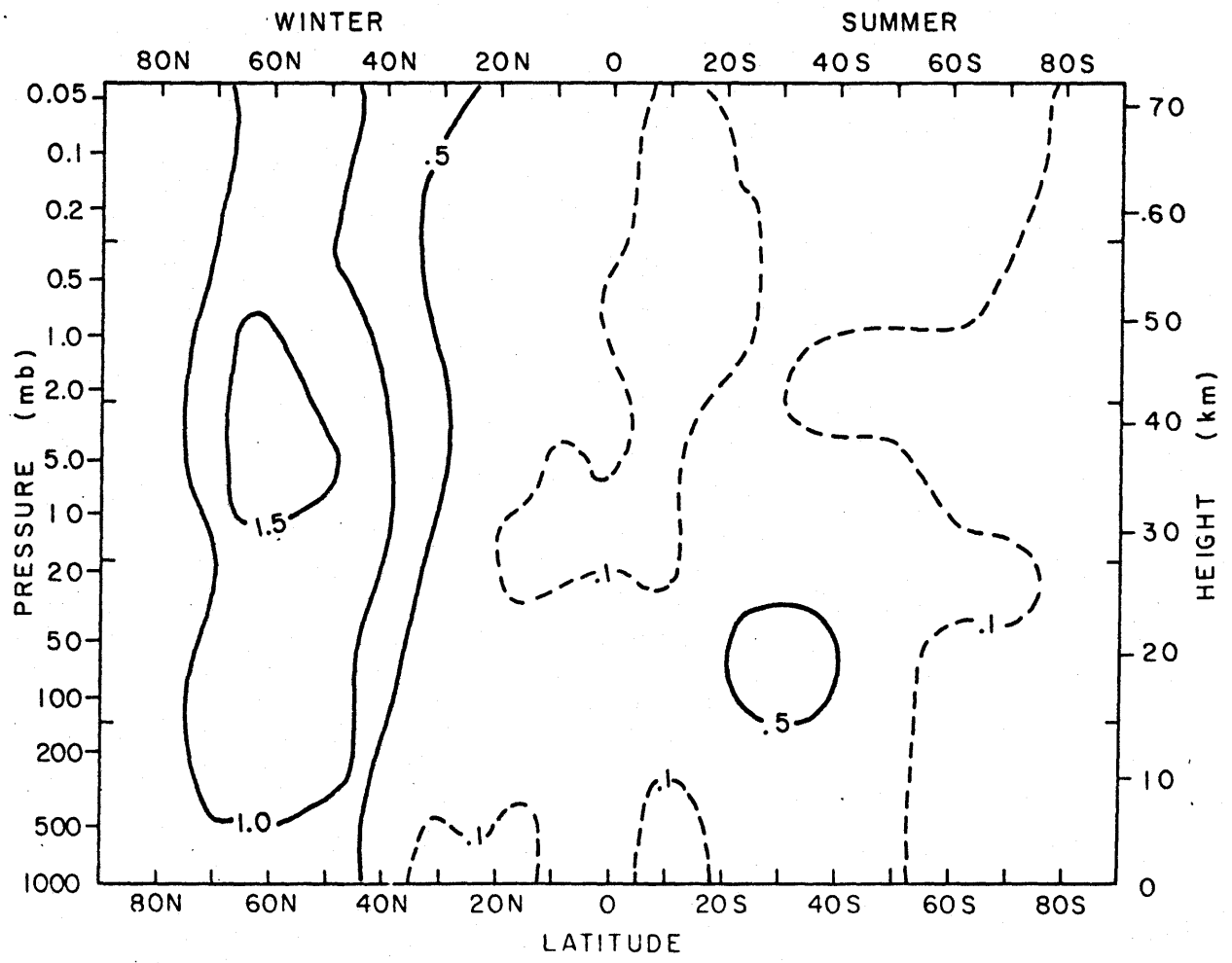

Figure 6.8: Amplitude of temperature wave-number 2 (in degrees Celsius) from satellite observations (winter-summer).

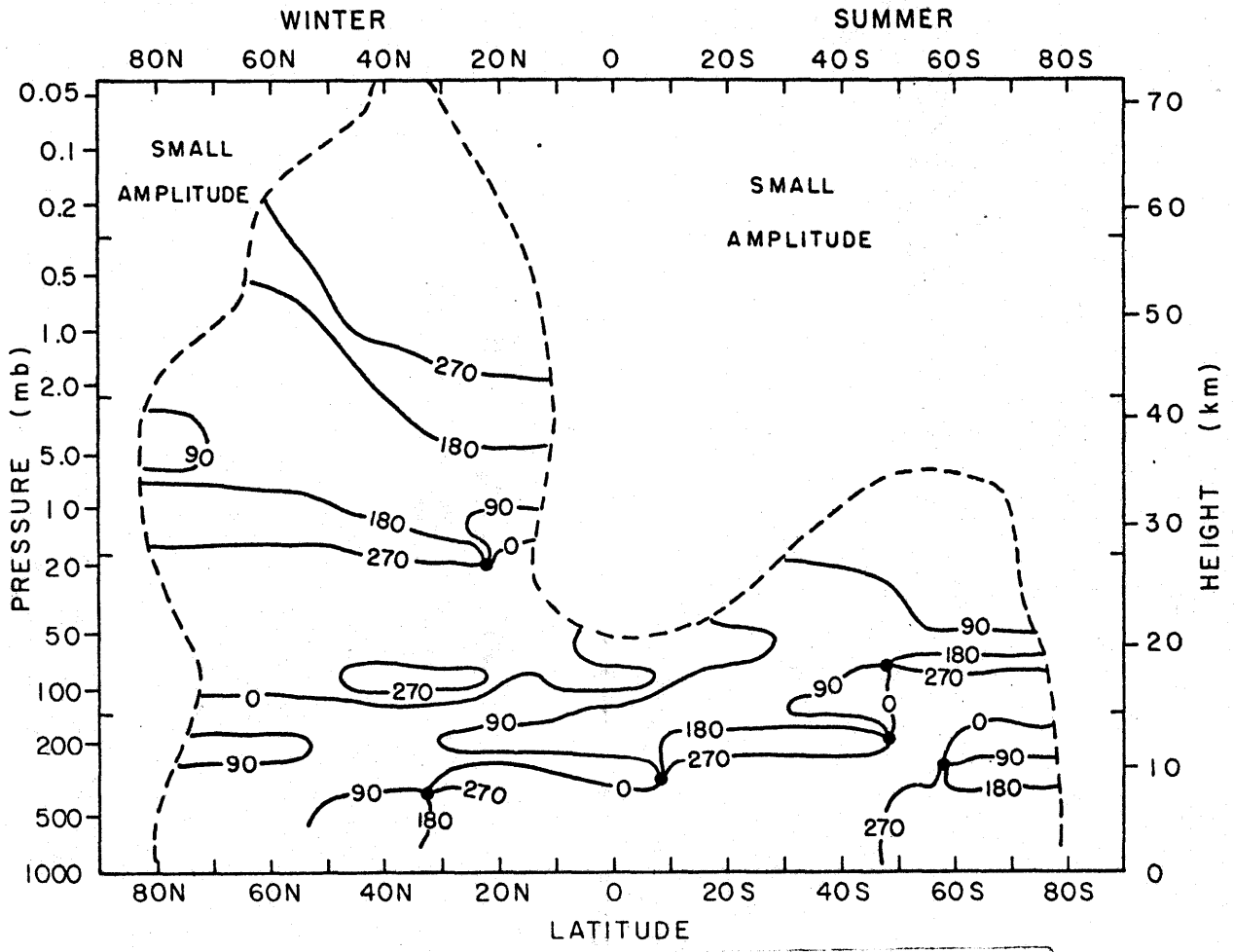

Figure 6.9: Phase (in degrees) of temperature wavenumber 3 from Run 29 (winter-summer).

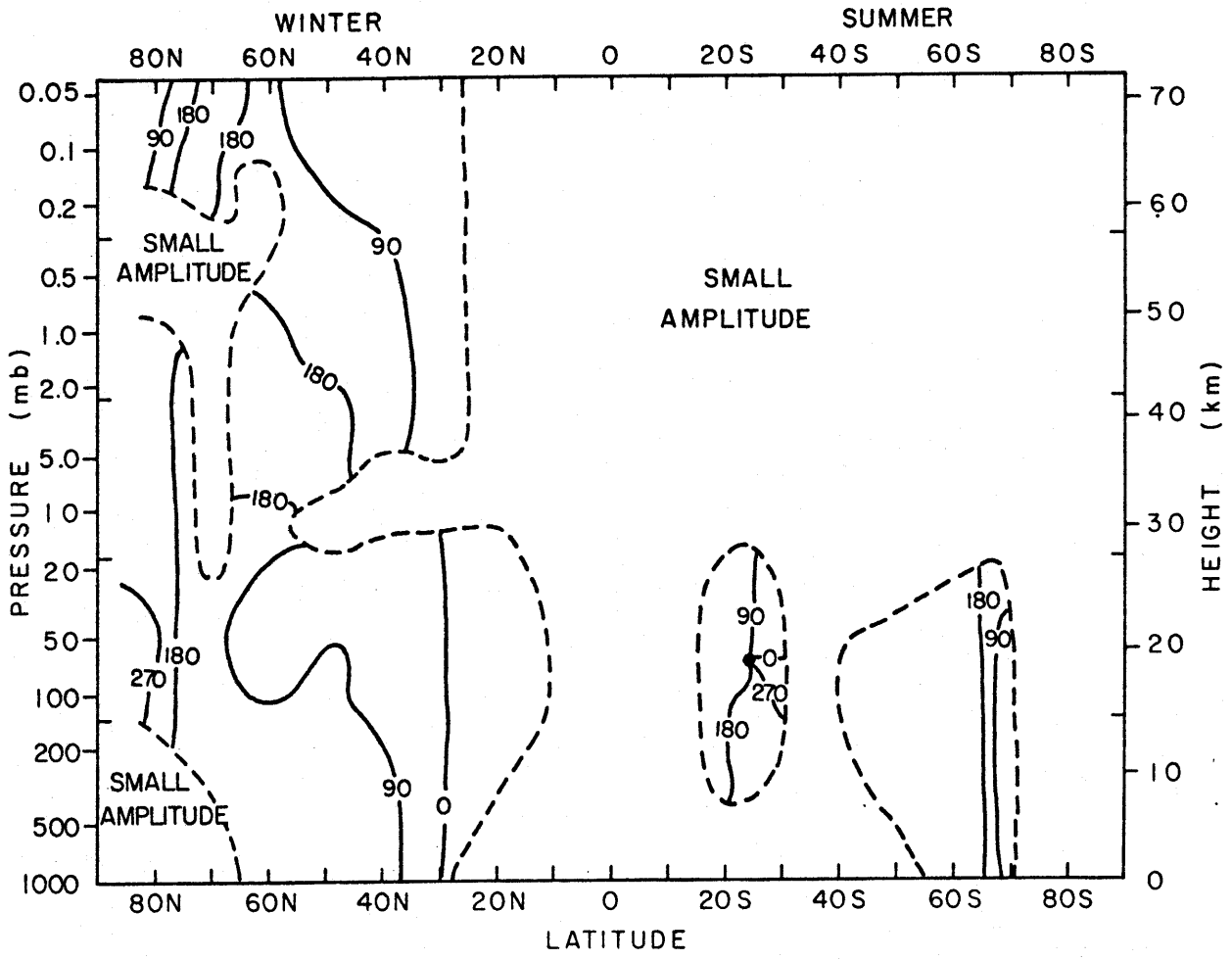

Figure 6.10: Phase (in degrees) of temperature wavenumber 3 from satellite observations (winter-summer).

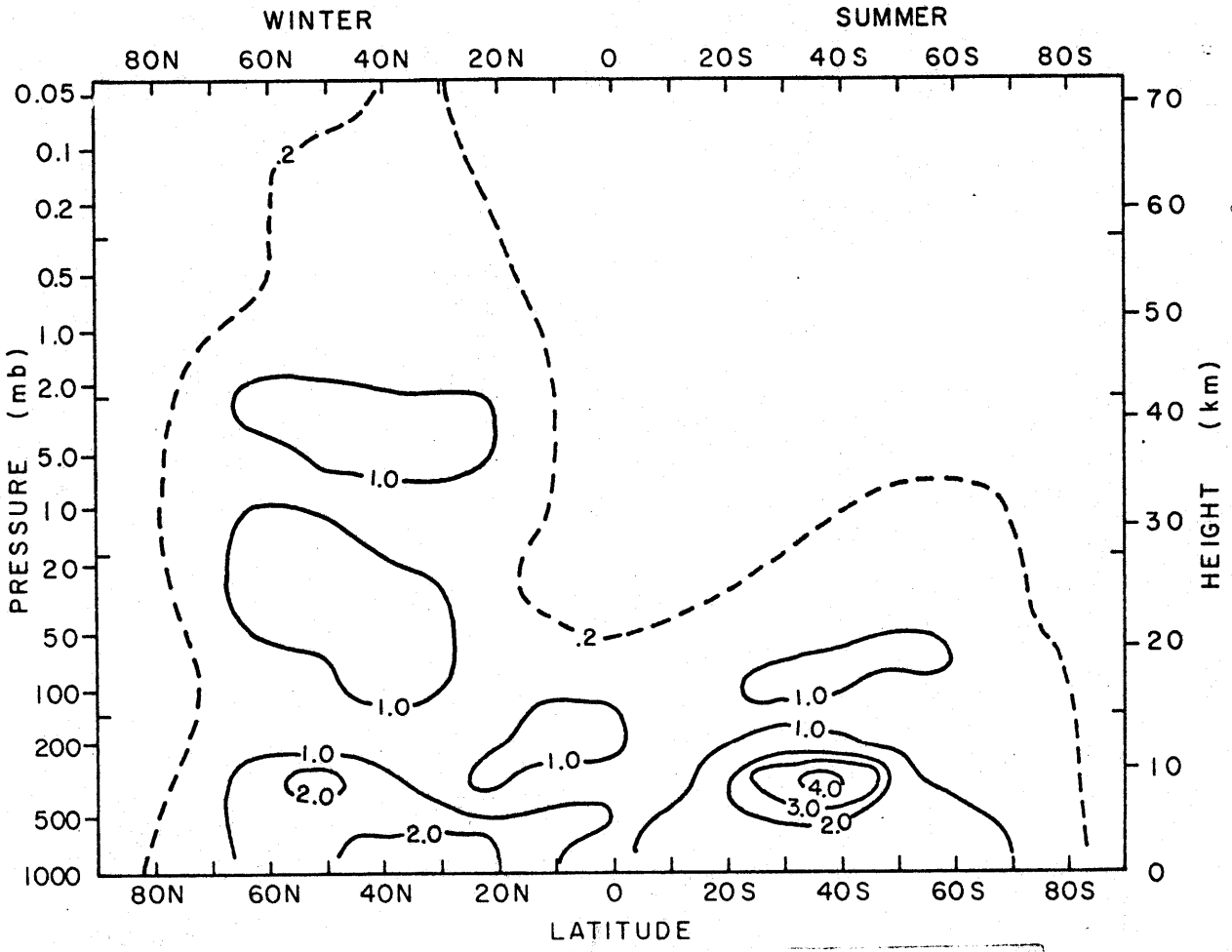

Figure 6.11: Amplitude of temperature wave-number 3 (in degrees Celsius) from Run 29 (winter-summer).

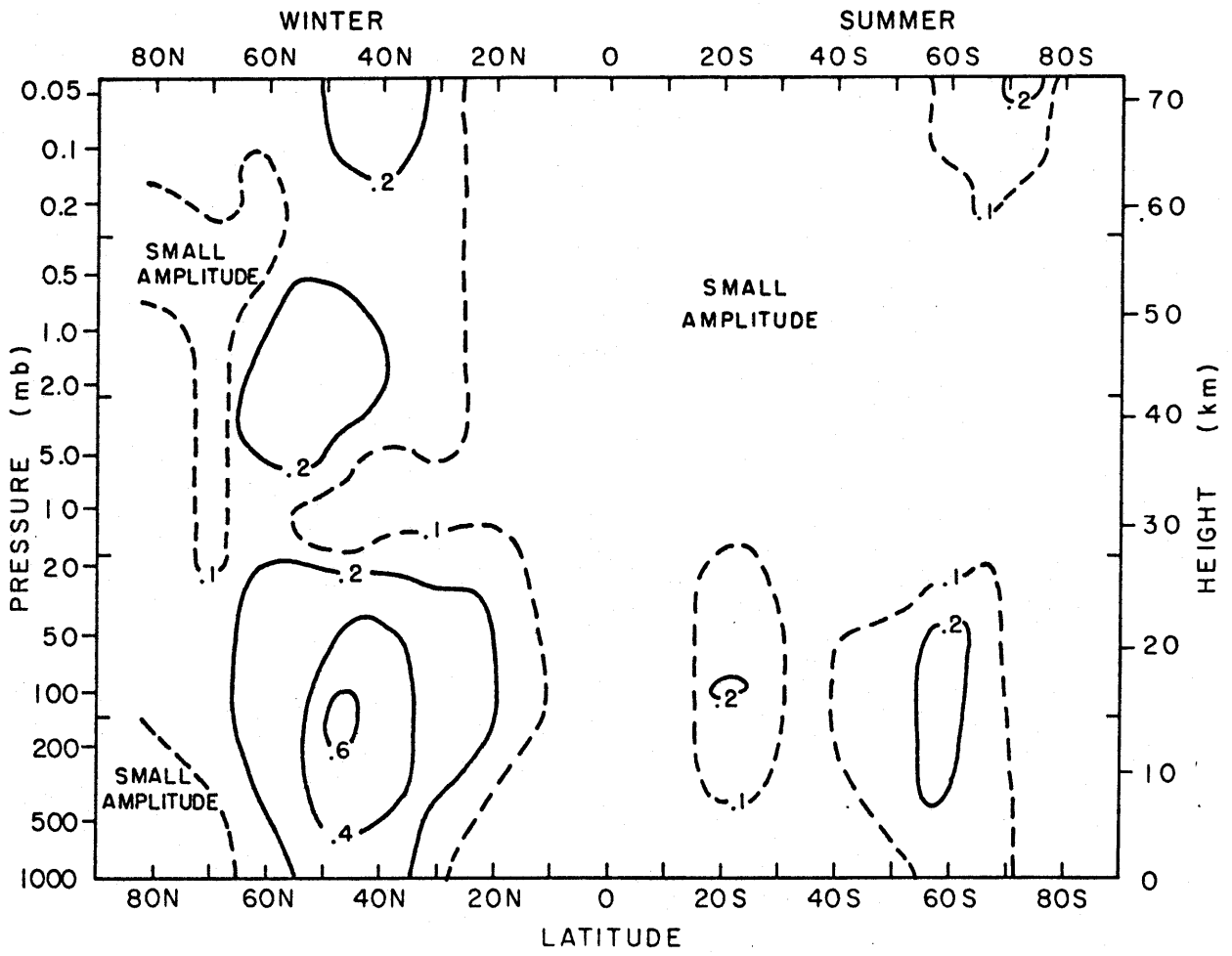

Figure 6.12: Amplitude (in degrees Celsius) of temperature wavenumber 3 from satellite observations (winter-summer).

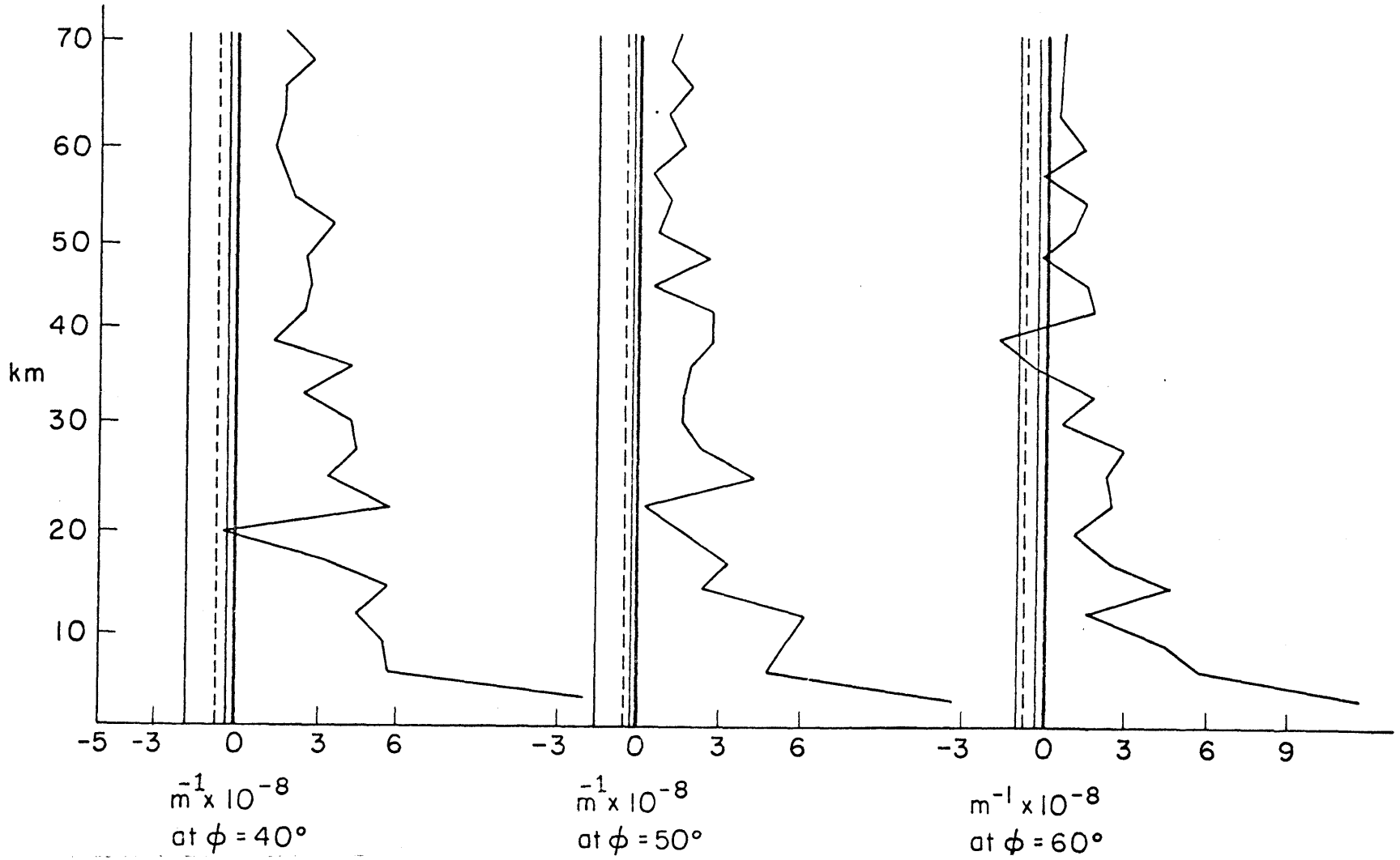

Figure 6.13: Comparison of terms in the equation for n^2 at three latitudes. Represented in each graph are, from left to right, $-(lNf^{-1})^2$, $-(2H)^{-2}$ (dotted line), $-(kNf^{-1})^2$, $N^2f^{-2}\bar{u}^{-1}(d\bar{q}/dy)$.

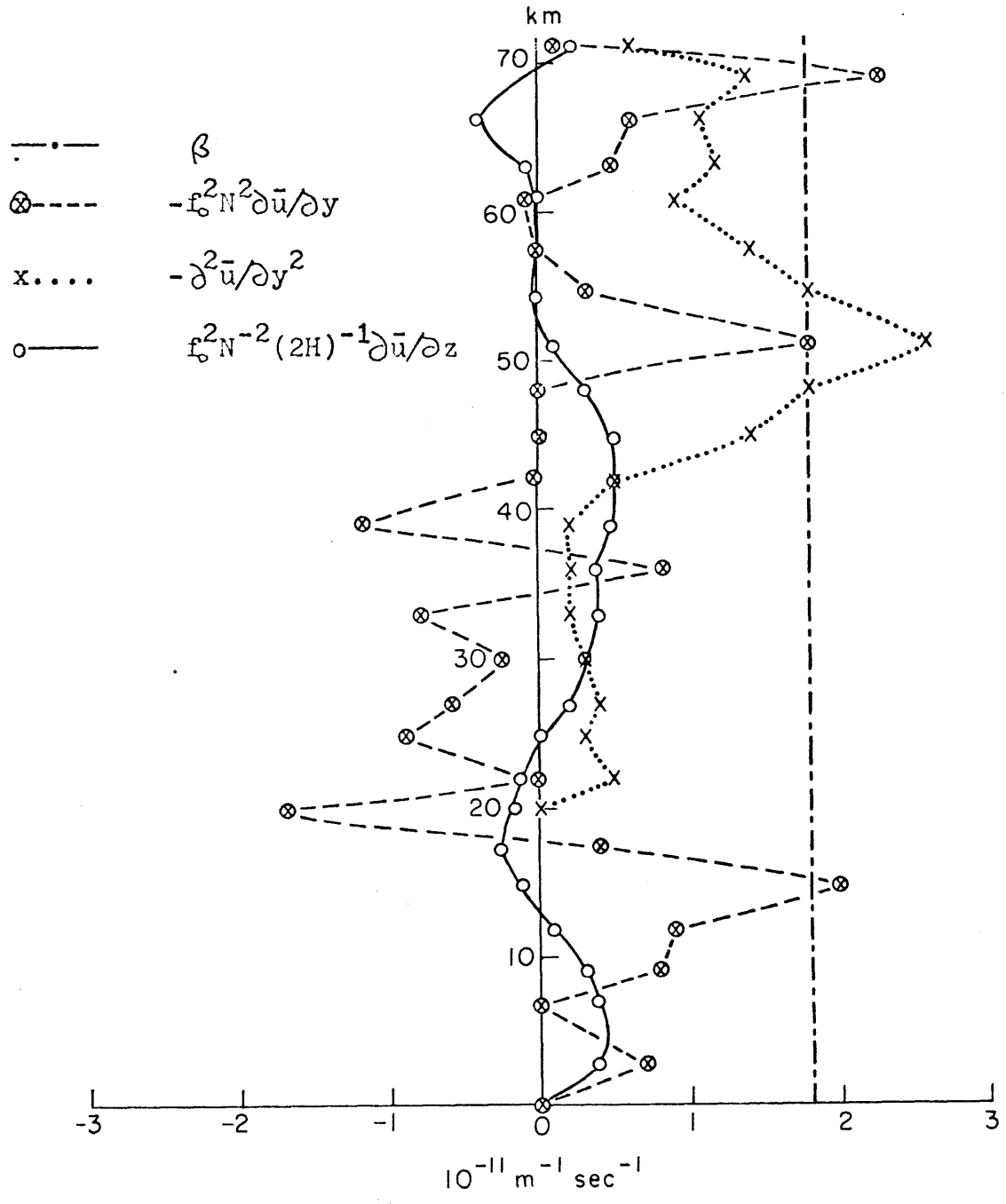

Figure 6.14: Comparison of terms in $d\bar{q}/dy$ at 40^{o}.

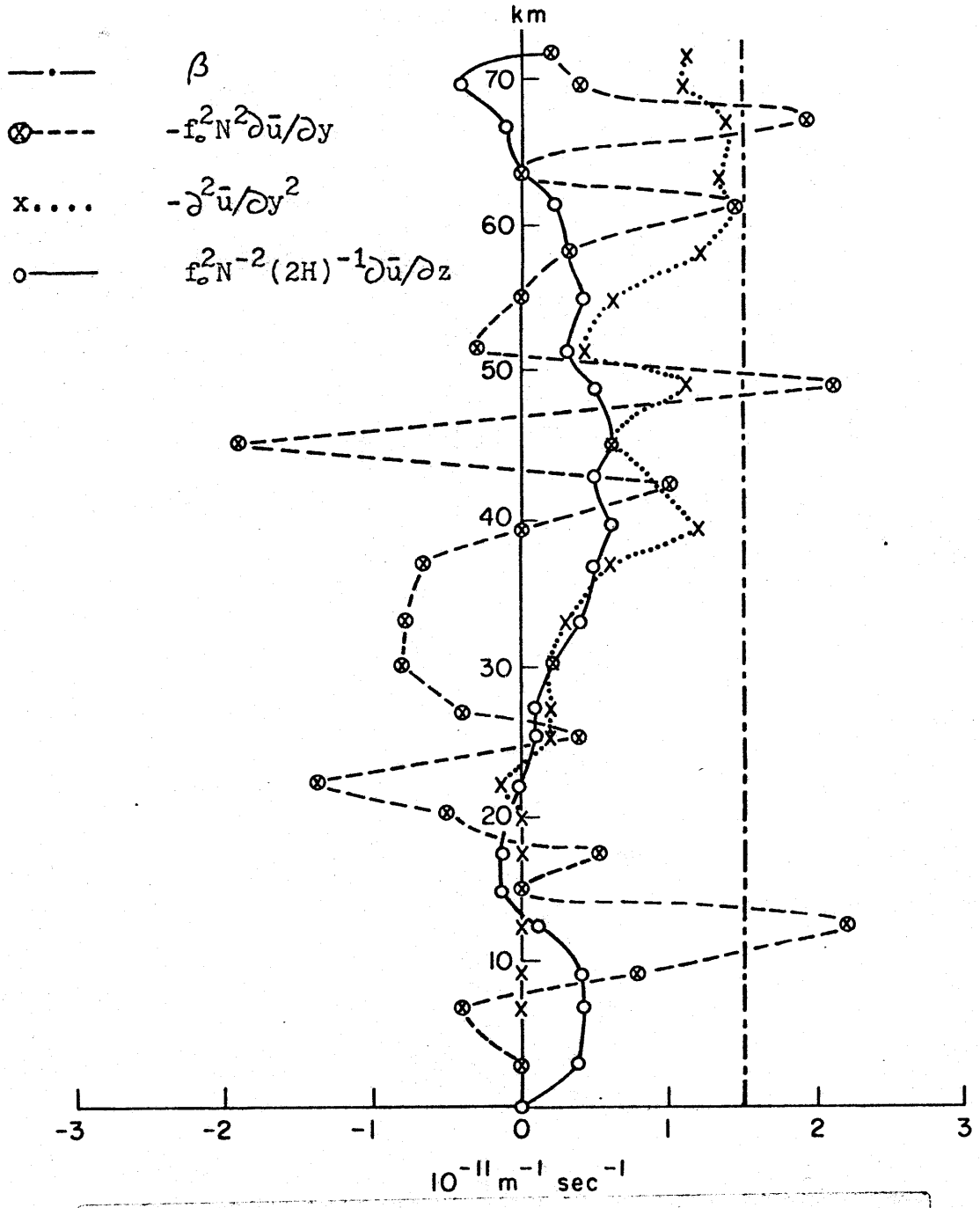

Figure 6.15: Comparison of terms in $d\bar{q}/dy$ at 50^o.

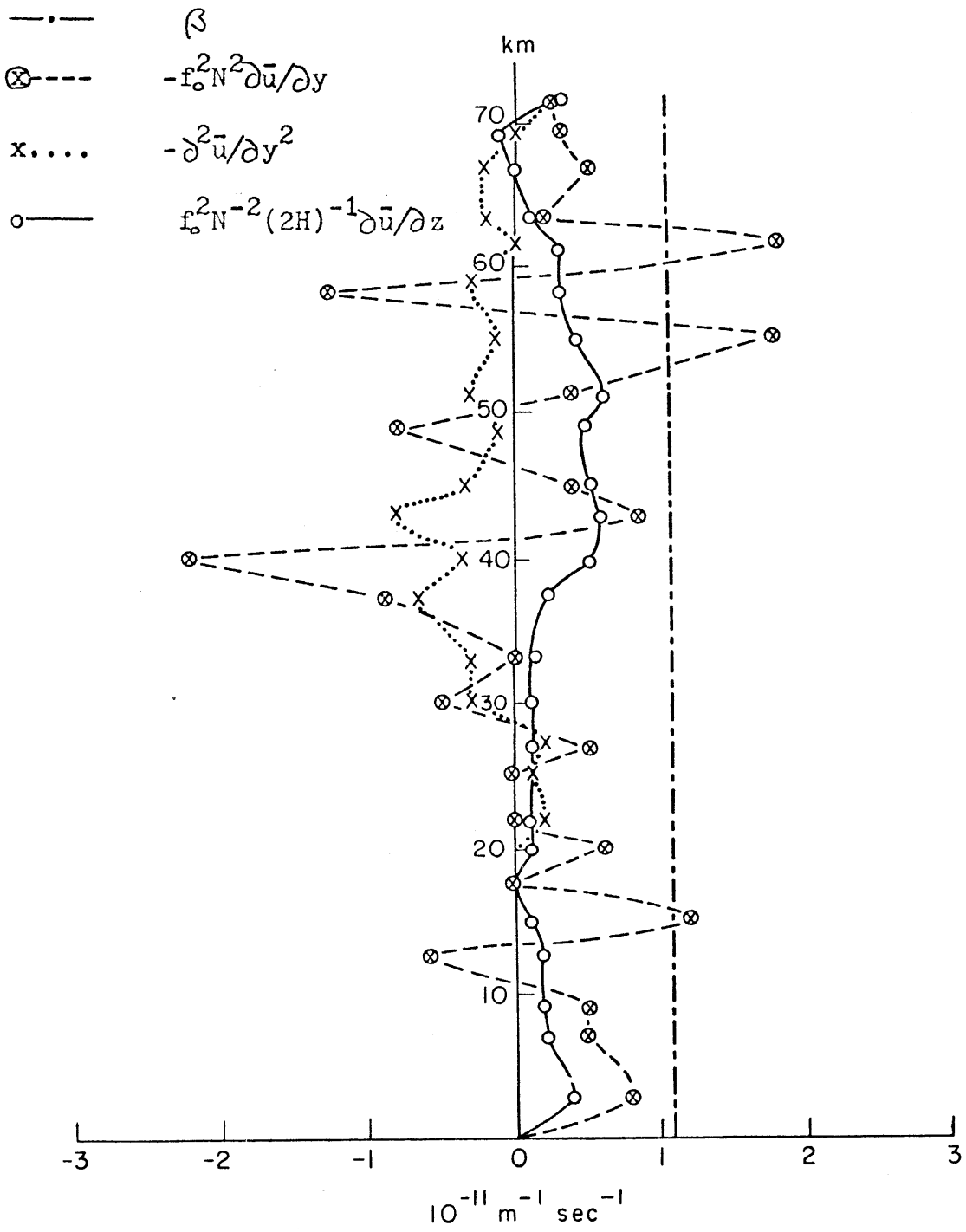

Figure 6.16: Comparison of terms in $d\bar{q}/dy$ at 60°.

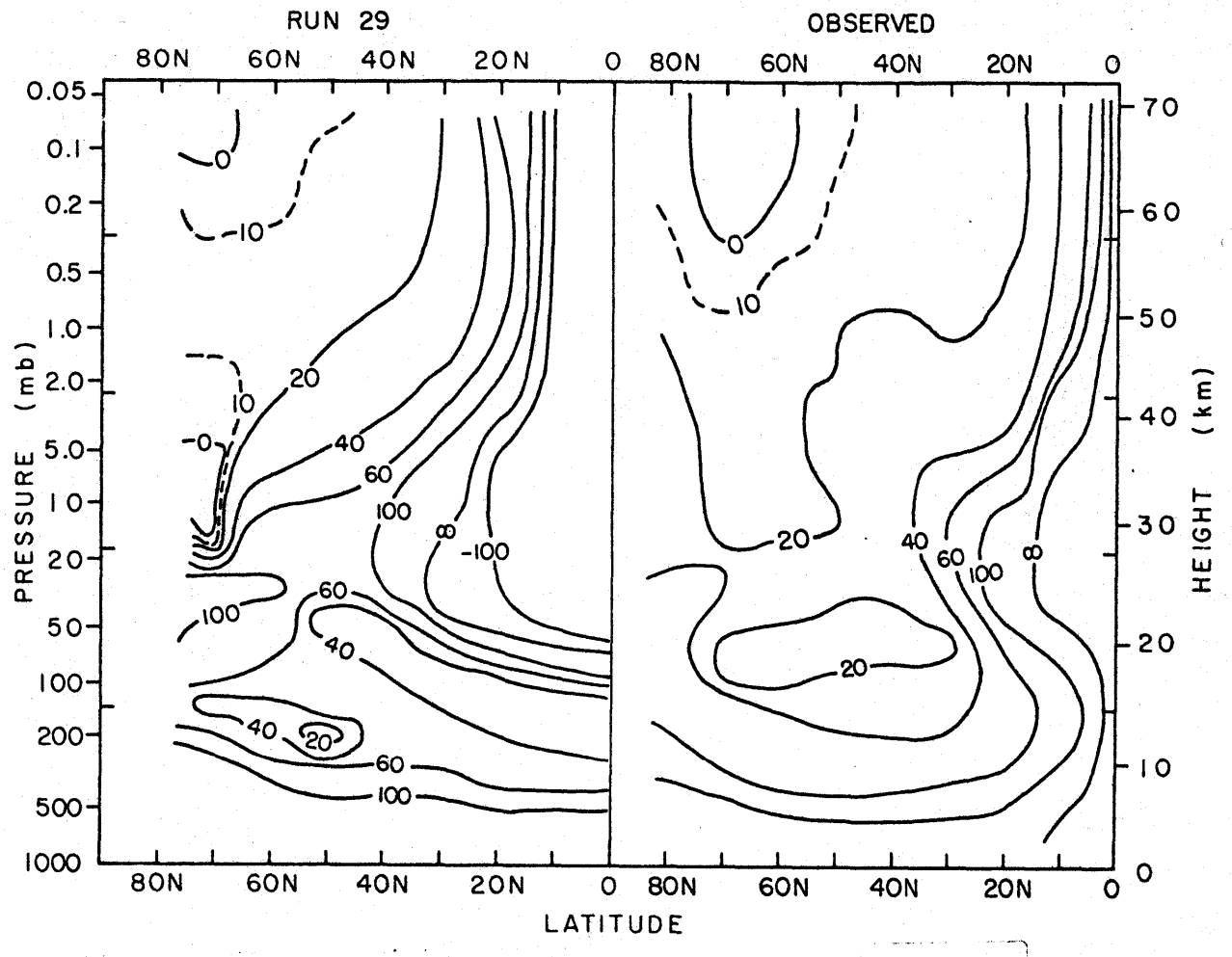

Figure 6.17: Matsuno formulation of refractive index squared (non-dimensional) for wavenumber 1 using wintertime mean zonal flow from Run 29 (left) and from Newell, 1968 (right).

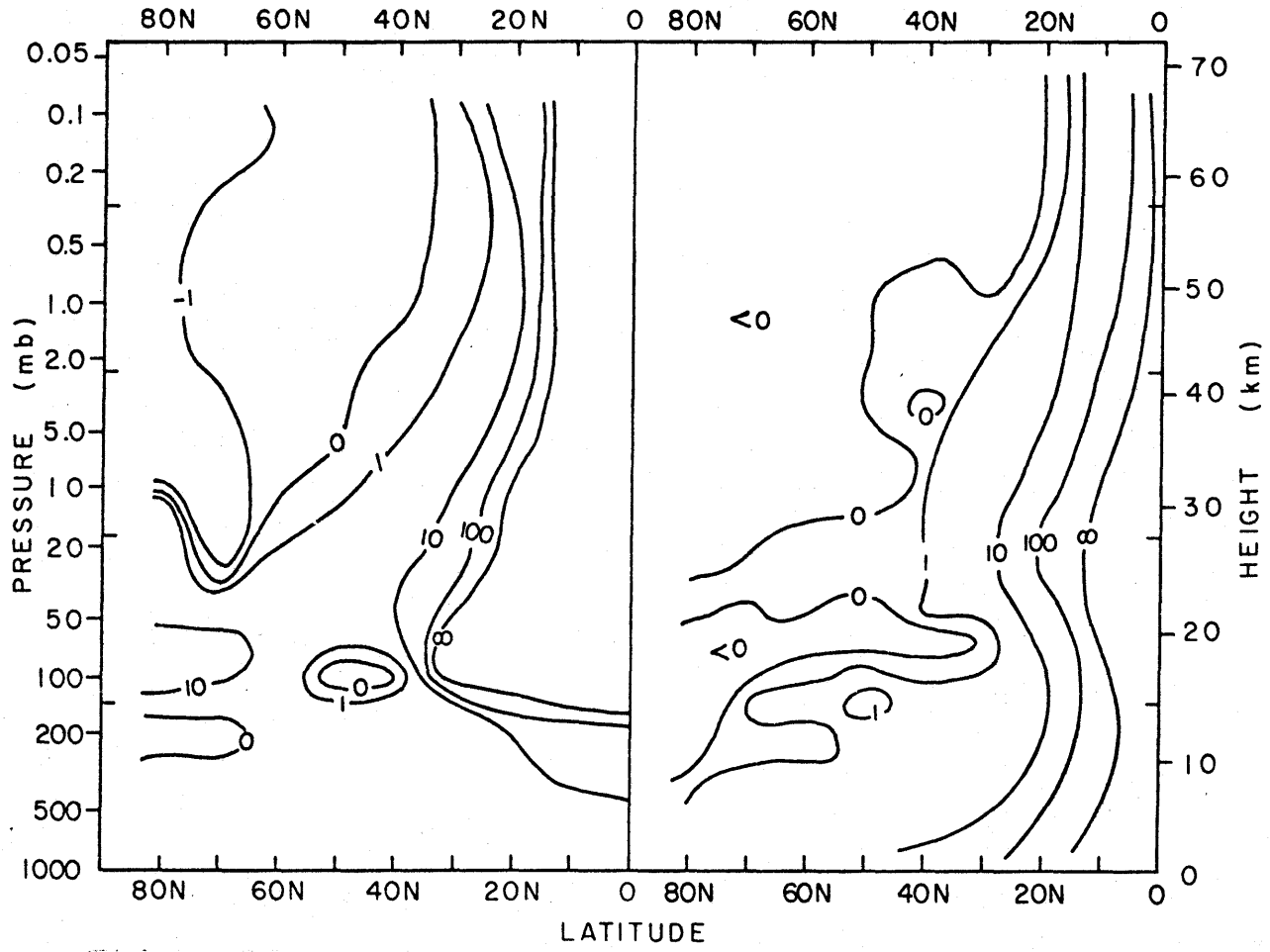

Figure 6.18: Charney-Drazin formulation of refractive index squared ($x10^{-8} m^{-1}$) for wavenumber 1 using the wintertime mean zonal flow from Run 29 (left) and from Newell, 1968 (right).

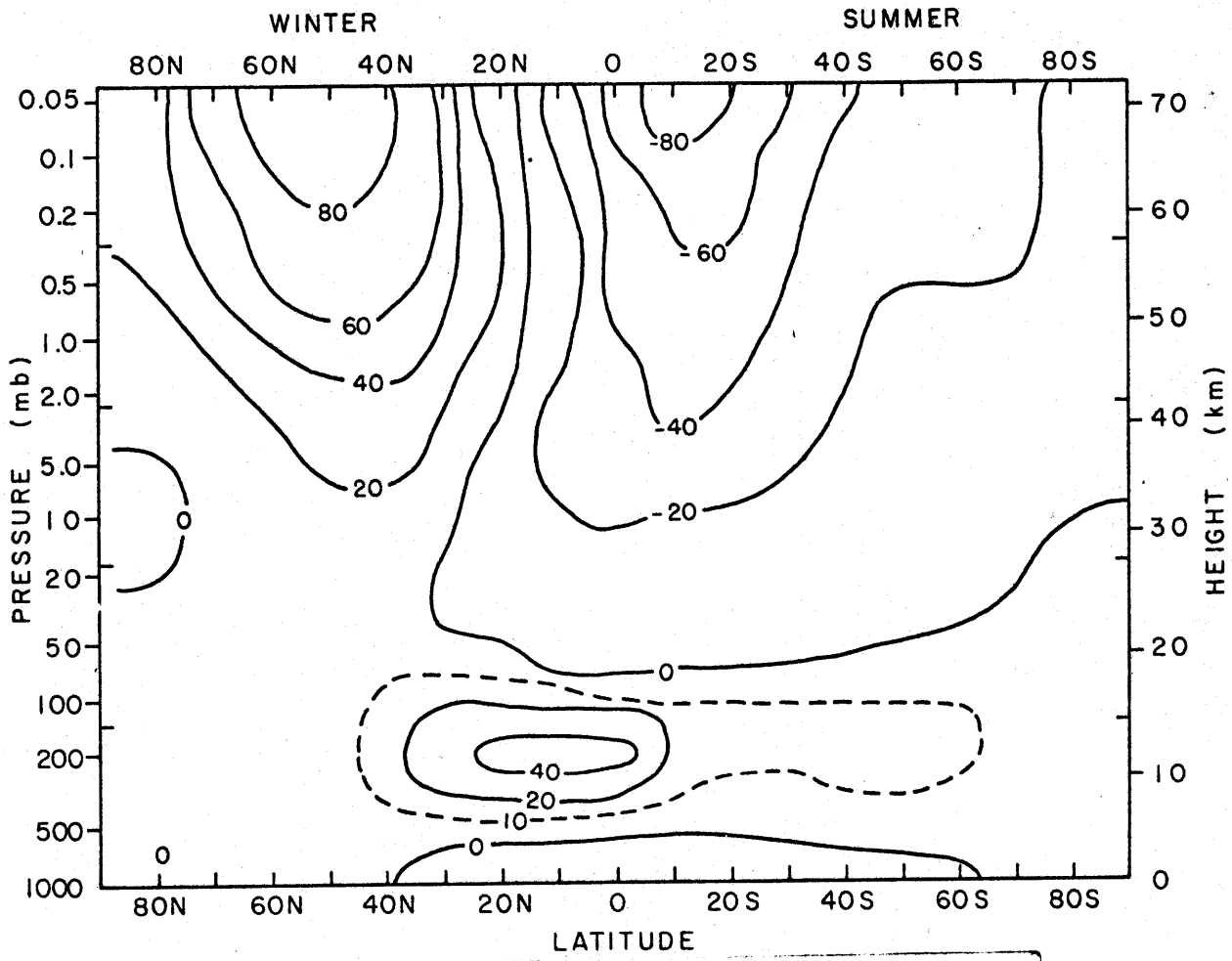

Figure 6.19: Winter-summer mean zonal wind from Run 29.

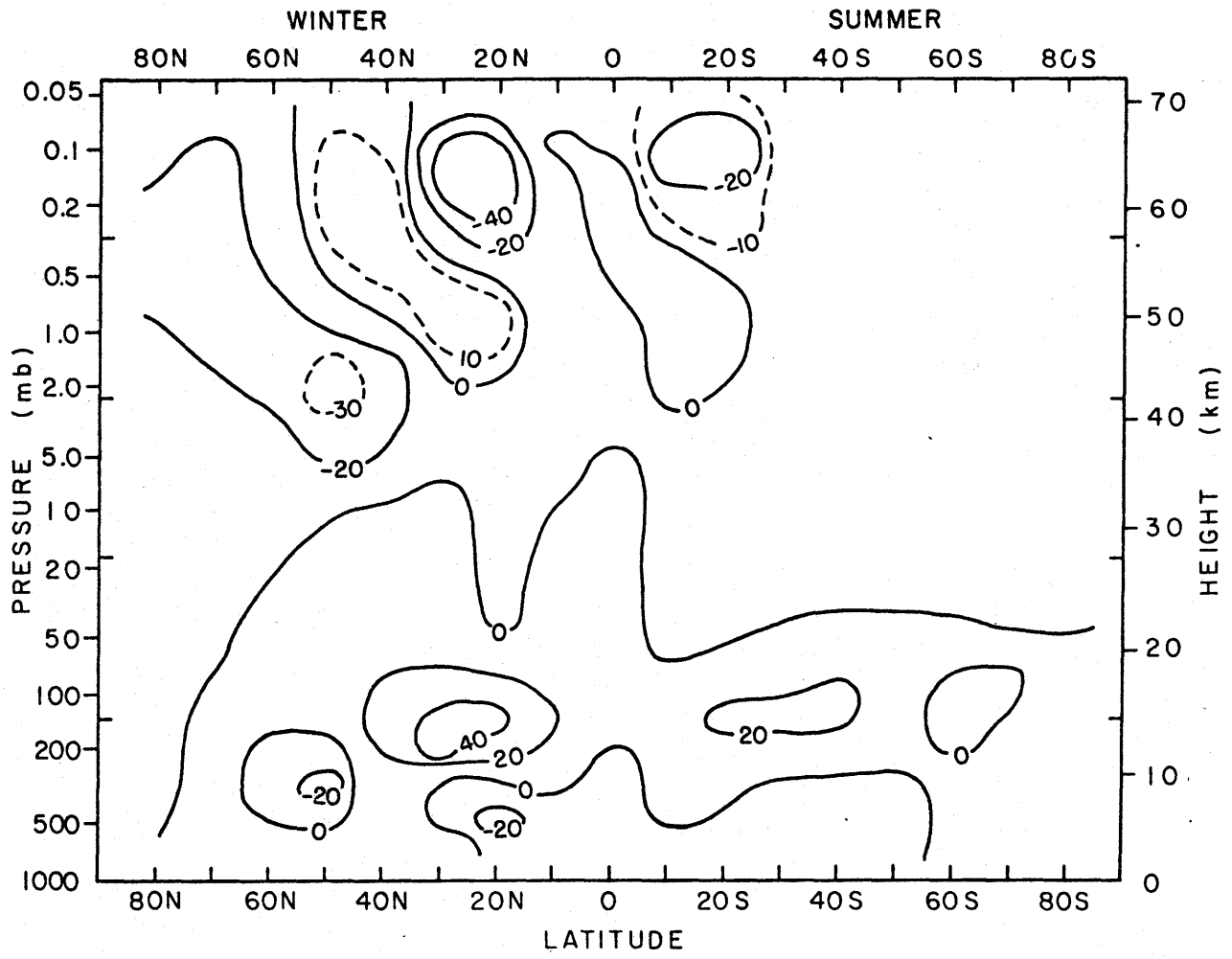

Figure 7.1: $\overline{((w^*u^*))}$ from Run 29 (winter-summer).

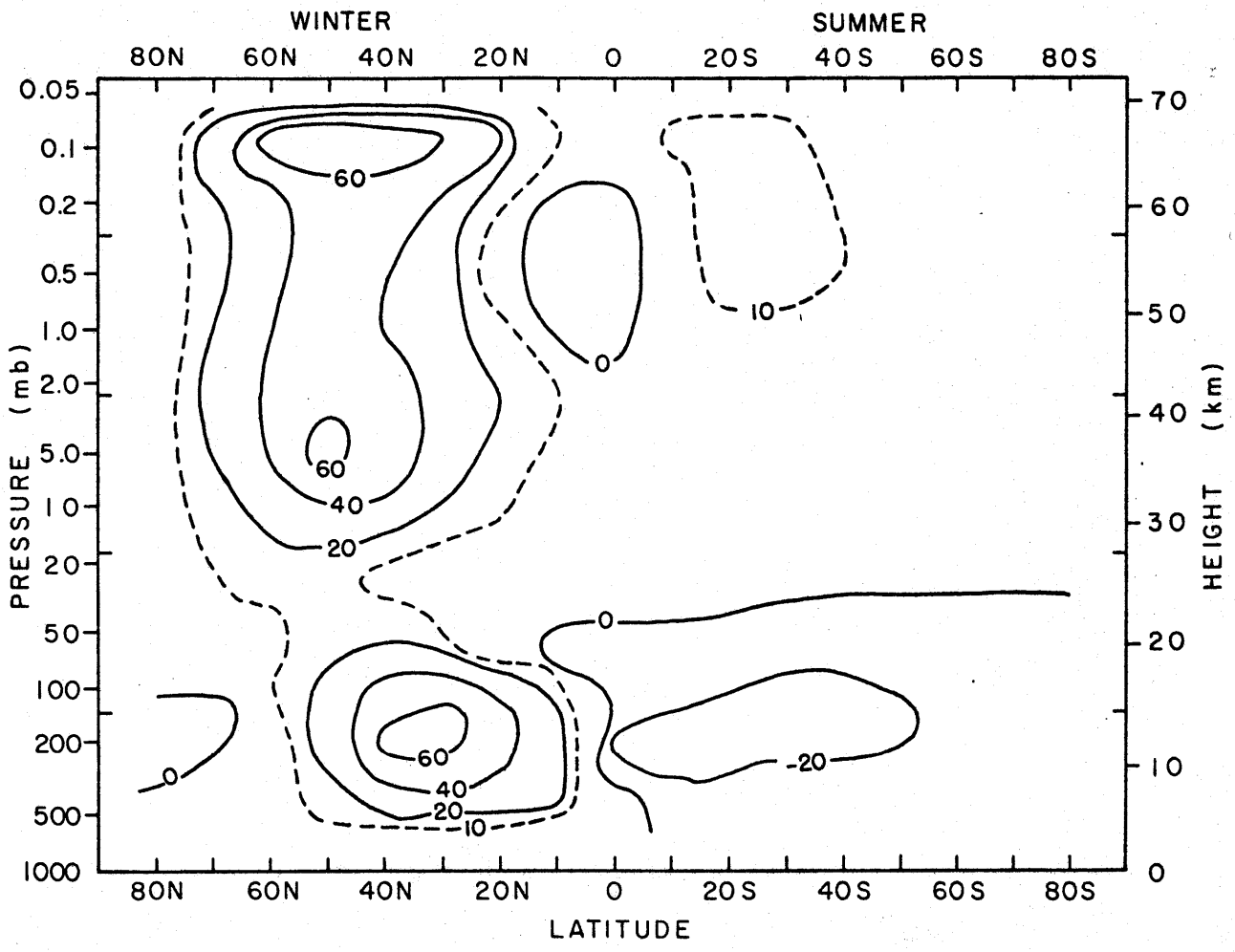

Figure 7.2: $\overline{((v^*u^*))}$ from Run 29 (winter-summer).